

Influence of initial soil moisture in a Regional Climate Model study over West Africa. Part 2: Impact on the climate extremes

Brahima KONÉ¹, Arona DIEDHIOU^{1, 2}, Adama Diawara¹, Sandrine Anquetin², N'datchoh Evelyne Touré¹, Adama Bamba¹ and Arsene Toka Koba¹

¹LASMES - African Centre of Excellence on Climate Change, Biodiversity and Sustainable Agriculture (ACE CCBAD) / Université Félix Houphouët Boigny, Abidjan, Côte d'Ivoire

²Univ. Grenoble Alpes, IRD, CNRS, Grenoble INP, IGE, F-38000 Grenoble, France

Correspondence to: Arona DIEDHIOU (arona.diedhiou@ird.fr)

Abstract.

The influence of the soil moisture initial conditions on climate extreme indices over West Africa is investigated using the fourth generation of Regional Climate Model version 4 (non-hydrostatic) coupled to the version 4.5 of the Community Land Model (RegCM4-CLM4.5) at 25 km spatial resolution. We initialized the control experiments with the reanalysis soil moisture of the European Centre Meteorological Weather Forecast's reanalysis of the 20th century data (ERA20C), while for the dry and wet experiments, we initialized the soil moisture at the maximum and minimum value over West Africa domain, respectively. For each experiment, an ensemble of five runs are performed for five years (2001- 2005), with soil moisture initial conditions prescribed on June 1 and simulations performed over four months (122 days) from June to September. The performance of RegCM4-CLM4.5 in simulating the ten extreme rainfall and temperature indices used in this study is presented. Then, the results are discussed for the two idealized simulations most sensitive to the dry and wet soil moisture initial conditions to highlight the impacts beyond the limits of soil moisture internal forcing in the model.

Over the Central Sahel, dry (wet) experiments lead to a decrease (increase) of precipitation extreme indices related to the number of events, not for those related to the intensity of the events. Soil moisture initial conditions unequally affect the daily minimum and maximum

32 temperatures. The strongest impact is found on the maximum temperature. Wet (dry)
33 experiments decrease (increase) maximum temperature in the whole region. Over the Central
34 Sahel, wet (dry) experiments lead to a decrease (increase) of the maximum values of minimum
35 temperature.

36

37 **1 Introduction**

38 West Africa experienced large rainfall variability during the late 1960s. This variability often
39 leads to flooding events, severe drought, and regional heatwaves, which have major economic,
40 environmental, and societal impacts (Easterling et al., 2000; Larsen, 2003). In recent years,
41 climate extremes have attracted much interest because they are expected to occur more
42 frequently (International Panel on Climate Change (IPCC), 2012) than changes in the mean
43 climate. Yan and Yang (2000) showed that for many cases, the extreme climate changes were
44 five to ten times greater than climate mean change. Many key factors or physical mechanisms
45 could be the cause of the increase in climate extremes (Nicholson, 1980; Le Barbé et al., 2002),
46 such as the effect of increasing greenhouse gases in the atmosphere on the intensification of hot
47 extremes (IPCC, 2007), sea surface temperature (SST) anomalies (Fontaine and Janicot 1996;
48 Folland et al., 1986), and land surface conditions (Philippon et al., 2005; Nicholson (2000)). In
49 addition, smaller-scale physical processes, including the interactions of land–atmosphere
50 coupling, can lead to changes in climate extremes. For the European summer, the influence of
51 soil moisture on land–atmosphere coupling using a regional climate model and focused on the
52 extremes and trends in precipitation and temperature have been studied by Jaeger and
53 Seneviratne (2011). For extreme temperatures, their studies have shown that interactions of soil
54 moisture and climate have a significant impact, while for extreme precipitation, they only
55 influence the frequency of wet days. Over Asia, Liu et al. (2014) studied the impact on
56 subsequent precipitation and temperature of soil moisture anomalies using a regional climate
57 model. They showed that wet (dry) experiences decrease (increase) the hot extremes, decrease
58 (increase) the drought extremes, and increase (decrease) the cold extremes in a zone with strong
59 soil moisture–atmospheric coupling. However, none of these studies examined the impacts of
60 the soil moisture initial conditions on subsequent climate extremes using a regional climate
61 model over West Africa. In part 1, the influence of initial soil moisture on the climate mean
62 was based on a performance assessment of the Regional Climate Model coupled with the
63 complex Community Land Model (RegCM4-CLM4.5) performed by Koné et al. (2018), where

64 the ability of the model to reproduce the climate mean has been validated. However, in Part 2,
65 before starting to study the influence of initial soil moisture on climate extremes, it was
66 necessary to assess the performance of RegCM4-CLM4.5 in simulating the ten temperature
67 indices and extreme rainfall events used in this study. This has never been done before in Africa;
68 therefore, we separated the work in two parts. The manuscript is organized as follows: Section
69 2 describes the RegCM4 model, experimental design, and methodology used in this study;
70 Section 3 presents the assessment of RegCM4-CLM4.5 in extreme climate simulation and the
71 impacts on climate extremes of the soil moisture initial conditions; and Section 4 documents
72 the conclusions.

73 **2. Model, experimental design and methodology**

74 **2.1 Model description and numerical experiments**

75 The fourth generation of the Regional Climate Model (RegCM4) of the International Centre for
76 Theoretical Physics (ICTP) is used in this study. Since this version, physical representations
77 have been subject to a continuous process of implementation and development. The release
78 used in this study was RegCM4.7. The non-hydrostatic dynamical core of the MM5 (Mesoscale
79 Model version 5, Grell et al., 1994) was ported to RegCM4 while maintaining the existing
80 hydrostatic core. RegCM4 is a limited-area model using a vertical grid sigma hydrostatic
81 pressure coordinate and a horizontal grid of the Arakawa B-grid (Giorgi et al., 2012). The
82 radiation scheme is from the NCAR-CCM3 (National Center for Atmospheric Research and
83 the Community Climate Model Version 3) (Kiehl et al., 1996), and the aerosol representation
84 is from Zakey et al. (2006) and Solmon et al. (2006). The large-scale precipitation scheme used
85 in this study is from Pal et al. (2000); the moisture scheme is called the SUBgrid EXplicit
86 moisture scheme (SUBEX), which considers the sub-grid variability in clouds. The accretion
87 and evaporation processes for stable precipitation are from Sundqvist et al. (1989). The sensible
88 heat and water vapour in the planetary boundary layer over land and ocean, as well as the
89 turbulent transport of momentum, is reported by Holtslag et al. (1990). The heat and moisture
90 and momentum of ocean surface fluxes are from Zeng et al. (1998). Convective precipitation
91 and land surface processes in RegCM4.7 are represented in several options. Based on Koné et
92 al. (2018), the convective scheme of Emanuel (1991) is used. The parameterization of land
93 surface processes is from CLM4.5 (Oleson et al., 2013). In each grid cell of CLM4.5, there are
94 sixteen different plant functional types and ten soil layers (Lawrence et al., 2011; Wang et al.,
95 2016). The integration of RegCM4 over the West African domain is shown in Fig. 1 with

182 × 114 grid points; from 20°W - 20°E and 5°S - 21°N). The European Centre for Medium-Range Weather Forecasts reanalysis (EIN75; Uppala et al., 2008; Simmons et al., 2007) provides the initial and boundary conditions. The sea surface temperatures (SSTs) are derived from the National Oceanic and Atmosphere Administration optimal interpolation weekly (NOAA; OI_WK) (Reynolds et al., 1996). The topography is derived from the United States Geological Survey (USGS) Global Multi-resolution Terrain Elevation Data (GMTED; Danielson et al., 2011) at a spatial resolution of 30 arc-s, which is an update of the Global Land Cover Characterization (GTOPO; Loveland et al., 2000) dataset.

We used the soil moisture from the reanalysis of the European Centre Meteorological Weather Forecast's Reanalysis of the 20th century (ERA20C) to initialize the control runs. Wet and dry experiments were initialized for the soil moisture at the maximum ($= 0.489 \text{ m}^3.\text{m}^{-3}$) and minimum ($= 0.117.10^{-4} \text{ m}^3.\text{m}^{-3}$) soil moisture values over West Africa derived from the ERA20C soil moisture dataset. In the part 1 of this study, we designed three experiments (reference, wet, and dry), each with a set of five (5) simulations starting from June 1st to September 30th. The difference between these three experiments is the change in the initial soil moisture condition (reference initial soil moisture condition, wet initial soil moisture condition, and dry initial soil moisture condition) during the first day of the simulation (June 1st, 2001, 2002, 2003, 2004, and 2005) over the West African domain. Then, we selected the two years most affected by the wet and dry initial soil moisture conditions (2003 and 2004) to estimate the limits of the impact of the internal soil moisture forcing on the new non-hydrostatic dynamic core of RegCM4.

For these two years most sensitive to soil moisture initial conditions, the Student t-test is used to compare the significance of changes in climate extreme indices between a wet or dry sensitivity test (sample 1) and the control (sample 2) in assuming that this method performs well for climate simulations (Damien et al., 2014) and knowing that it is extensively used for climatological analysis (Menedez et al., 2019; Talahashi and Polcher, 2019). In this study, the t-test at the 95% confidence level was used to consider statistically significant.

124

125 **2.2 Validation datasets and evaluation metrics**

126 Our investigation focused on the air temperature at 2 m and the precipitation over the West
127 African domain during JJAS for 2003 and 2004. The simulated precipitation fields are validated

128 with the Climate Hazards Group Infrared Precipitation Stations (CHIRPS) dataset from the
129 University of California at Santa Barbara, available from 1981 to 2020 with 0.05° high-
130 resolution data. We have chosen CHIRPS as reference in this study, mainly because this
131 product has been widely assessed and used for the study of extreme events in West Africa by
132 Bichet et al. (2018a, b) and Didi et al. (2020).

133 We validated the 2-m temperature using the The National Oceanic and Atmospheric
134 Administration (NOAA) Climate Prediction Center (CPC) daily maximum and minimum
135 global surface air temperature. The NOAA/CPC global daily surface 2-m air temperature (CPC-
136 T2m) is a land-only gridded global daily maximum (Tmax) and minimum (Tmin) temperature
137 analysis from 1979 to the present, available at two spatial of $10 \text{ min} \times 10 \text{ min}$ and $0.5^\circ \times 0.5^\circ$
138 (latitude \times longitude). This product provides an observational T2m estimate for climate
139 monitoring, model evaluation, and forecast verification (Fan Y. and Huug van den Dool, 2008;
140 Pan et al., 2019). In this study, the daily Tmax and Tmin are used at spatial resolution $0.5^\circ \times$
141 0.5° . To compare the model simulations with the observation datasets, we re-gridded all the
142 products to $0.22^\circ \times 0.22^\circ$ using a bilinear interpolation method (Nikulin et al., 2012).

143 The performance of RegCM4-CLM4.5 to simulate the extreme indices is evaluated using four
144 selected sub-regions (Fig. 1) based on the previous work of Koné et al. (2018), which
145 correspond to different annual precipitation cycle features. We used the mean bias (MB), which
146 captures the small-scale differences between the simulation and observation. The pattern
147 correlation coefficient (PCC) is also used as a spatial correlation between model simulations
148 and observations to indicate the large-scale similarity degree.

149 To quantify the impact of soil moisture initial conditions on climate extremes over Asia, Liu et
150 al. (2014) used the MBs in five subregions. In our study, we used the MBs and the probability
151 density functions (PDF, Gao et al. (2016); Jaeger and Seneviratne (2011)) for this purpose to
152 better capture how many grid points are impacted by initial soil moisture and their highest value.

153
154
155

156 **2.3. Extreme rainfall and temperature indices**

157 In this study, we investigated the changes in precipitation and temperature in terms of duration,
158 occurrence, and intensity of six extreme rainfall and four extreme temperature indices using
159 daily rainfall and daily minimum and maximum temperature data (Table 1). These ten extreme

160 indices are recommended by the Expert Team on Climate Change= Detection and Indices
161 (ETCCDI, Peterson et al., 2001).

162 **3. Results and discussion**

163 **3.1. Seasonal extreme rainfall**

164 In this section, we analyzed six extreme rainfall indices based on daily precipitation in RegCM4
165 simulations over West Africa. All precipitation indices were calculated for JJAS in 2003 and
166 2004. Table 2 summarizes the PCC and the MB of all precipitation indices studied in this
167 section for simulations obtained from control experiments with respect to CHIRPS
168 observations, calculated for the West Sahel, Central Sahel, Guinea Coast, and the entire West
169 African domain during the runs JJAS 2003 and JJAS 2004

170

171 **3.1.1 The number of the wet days (R1mm)**

172 Figure 2 shows the mean values of the number of wet days (R1mm, in days) from CHIRPS
173 (Fig. 2a, c) observation and the simulated control experiments (Fig. 2b, d) with the initial soil
174 moisture derived from ERA20C reanalysis. The R1mm index maximum values up to 100 days
175 in CHIRPS observation are found over mountainous regions such as the Cameroon Mountains,
176 Jos Plateau, and Guinea Highlands, while minimum values less than 50 days are found over the
177 Sahel and along the coastline from Liberia to Ghana with the number of wet days decreasing
178 gradually from south to north.

179 The control experiments (Fig. 2b, d) reproduce well the large-scale pattern of the observed
180 rainfall, with PCC values of 0.96 and 0.95 for runs JJAS 2003 and JJAS 2004, respectively
181 (Table 2) over the entire West African domain, but exhibit some spatial extent and magnitude
182 biases at local scale. The control experiments display a large and quite homogeneous area of
183 maximum values of R1mm index below 12 °N latitude and overestimate the number of wet
184 days over most of the studied domains (Table 2). The largest MBs are found over the Guinea
185 Coast with MB values more than 53.16 and 55.46 days for the runs JJAS 2003 and JJAS 2004,
186 respectively (Table 2). This overestimation of the number of wet days in RegCM4 is also found
187 by Thanh et al. (2017) with RegCM4 for Asia.

188 Figure 2 (second panel) displays additional changes in the R1mm index for JJAS 2003 and
189 JJAS 2004 from the dry (Fig. 2e and g) and wet experiments (Fig. 2f and h) compared to the
190 control experiments; the dotted area shows changes with statistical significance at the 95%
191 level. The dry experiments (Fig. 2e, g) decrease the R1mm index values, while the wet

192 experiments (Fig. 2h, j) increase them, especially over Central Sahel. However, over the Guinea
193 Coast sub-region, both wet and dry experiments show a significant increase in R1mm index
194 values.

195 For a better quantitative evaluation, Figure 3 displays the PDF distributions of changes in
196 R1mm over the sub-domains (Fig. 1), during the runs JJAS 2003 and JJAS 2004 while Table 3
197 summarizes the PDF maximum values. The results essentially confirm the linear impact found
198 over Central Sahel (Fig. 3a). Over West Sahel, the Guinea Coast, and the West African domain
199 (Fig. 3b, c, and d), both dry and wet experiments increase the R1mm index values. The strongest
200 R1mm increase is found in wet experiments over West Sahel, with a maximum change about
201 12 days in JJAS 2003 (Table 3) while the strongest R1mm decrease is found for dry experiments
202 over Central Sahel, with a maximum change about -5.19 days (Table 3).

203 .
204 Summarizing the results of this section, RegCM4 overestimated the number of wet days over
205 most of the studied domains. Over the Central Sahel, wet and dry experiments lead both to a
206 linear impact on the R1mm index with an increase and a decrease respectively of the number
207 of rainy days. These results are compatible with previous work that sustained a strong land–
208 atmosphere coupling in transition areas between wet and dry climate regimes (Zhang et al.,
209 2011; Koster et al., 2006).

210

211 **3.1.2 Simple daily intensity index (SDII).**

212 We analyzed in this section the SDII index (rainfall intensity in $\text{mm}\cdot\text{day}^{-1}$) which gives the
213 amount of precipitation mean on total wet days (daily precipitation $>1\text{mm}$). Figure 4 (first
214 panel) is the same as figure 2 (first panel) but for the rainfall intensity. Over the coastline of
215 Guinea Coast, CHIRPS observation (Fig.4a, c) depicted the highest values of SDII index, more
216 than $25\text{mm}\cdot\text{day}^{-1}$. While, over the Sahel and Sahara, CHIRPS observation showed large extend
217 SDII index values not exceeding $12\text{mm}\cdot\text{day}^{-1}$ in both runs JJAS 2003 and JJAS 2004.

218 The control experiments (Fig. 4 b, d) reproduced well the large-scale pattern of CHIRPS with
219 PCC values reaching 0.73 and 0.77 (in the runs JJAS 2003 and JJAS 2004, respectively; Table
220 2) over the West African domain. However, at the local scale, some biases are found. Over most
221 of the studied domains, the magnitude of the SDII is underestimated and not exceed $10\text{mm}\cdot\text{day}^{-1}$,
222 excepted over the Cameroon Mountains (Fig. 4b, d). The largest MB values were located
223 over the Guinea Coast with MB values greater than -13.62 and $-14.65\text{mm}\cdot\text{day}^{-1}$ for the runs
224 JJAS 2003 and JJAS 2004, respectively (Table 2).

225 Figure 4 (second panel) is the same as figure 2 (second panel) but for the rainfall intensity.
226 Unlike the R1mm index, changes in the SDII index due to soil moisture initial conditions are
227 not linear over most of studied domains. Fig. 4 (second panel) shows that generally, the impact
228 on rainfall intensity of dry and wet experiments presents areas of increase and decrease over
229 most of the studied sub-domains.

230 Figure 5 displays PDFs of changes in SDII, as in Fig. 3. The PDFs show a maximum change
231 value centered approximately on zero (Table 3), indicating that changes in the rainfall intensity
232 for wet and dry experiments are not significant.

233 In summary, RegCM4 underestimates the rainfall intensity over the studied domain compared
234 to the observation and the impact on SDII index in wet and dry experiments are not significant.

235

236 **3.1.3 Maximum number of consecutive dry days (CDD).**

237 The duration of consecutive dry days (CDD, in days), which represents the maximum number
238 of consecutive dry days with precipitation less than $1 \text{ mm}\cdot\text{day}^{-1}$ is analyzed in this subsection.
239 Figure 6 (first panel) is the same as figure 2 (first panel) but for CDD. CHIRPS observation
240 locates the highest CDD values over the Sahara, with length more than 50 days (Fig. 6a, c). The
241 lowest CDD values are found over the Guinea Coast, with length less than 8 days.

242 The control experiments (Fig. 6b, d) over the entire West African domain well reproduce the
243 large-scale pattern of the observed rainfall with a PCC values more than 0.85 and 0.89 for the
244 runs JJAS 2003 and JJAS 2004, respectively (Table 1). However, in terms of magnitude, some
245 differences are observed at local scale. In general, the control experiments overestimate the
246 CDD over most of studied subdomains, except over the Guinea Coast (Table 2). The strongest
247 overestimation is found over West Sahel with MB values reaching more than 14.49 and 17.51
248 days for runs JJAS 2003 and JJAS 2004, respectively (Table 2). The current model
249 parameterization increases the drought extreme over most of the studied domains, except over
250 the Guinea Coast (Table 2).

251 Figure 6 (second panel) is the same as figure 2 (second panel) but for CDD. The soil moisture
252 initial condition impact on CDD index is linear over the Central and West Sahel (Fig. 6, second
253 panel); Over the Sahel, dry (wet) experiments increase (decrease) the length of dry spells. Over
254 the Guinea Coast, the impacts on CDD are weak for both dry and wet experiments and in
255 average, soil moisture initial conditions seems to decrease the length of dry spells in a central
256 band between Côte d'Ivoire and Nigeria.

257 Figure 7 is the same as figure 3 but displays the PDF distribution of the changes in CDD. The
258 highest length of CDD increase are found over the Central Sahel in dry experiments with
259 maximum change in length reaching 3.80 days in JJAS 2004 (Table 3), while the highest CDD
260 decrease are found over West Sahel in wet experiments with maximum change in length
261 reaching -12.73 days in the run JJAS 2003 (Table 3).

262 In summary, RegCM4 overestimated the maximum number of consecutive dry days over most
263 studied subdomains, except over the Guinea Coast. However, the impact of soil moisture initial
264 condition is linear over the Central and West Sahel. Over the Guinea Coast, the dry and wet
265 experiments generally decrease the length of dry spells.

266

267 **3.1.4 Maximum number of consecutive wet days (CWD).**

268 The duration of wet spells (CWD) which represents the maximum number of consecutive wet
269 days with precipitation $\geq 1 \text{ mm}\cdot\text{day}^{-1}$ is investigated in this subsection. Figure 8 (first panel) is
270 the same as figure 2 (first panel) but shows the CWD duration. In the CHIRPS observation, the
271 maximum length of CWD lasting longer than 20 days are found over the mountain regions such
272 as Cameroon Mountains, Jos plateau and Guinea highlands. While the minimum length of
273 CWD lasting less than 4 days are found over most of the area above the latitude 17°N (Fig.8a,
274 c).

275 The control experiments well reproduce the large-scale pattern over the entire West African
276 domain, with PCC values around 0.81 and 0.87 (resp. for JJAS 2003 and JJAS 2004, Table 2).
277 However, at local scale, the control experiments exhibit some biases in the CWD minimum and
278 maximum values, both in terms of magnitude and spatial extent. Control experiments
279 overestimate the CWD length over most of subdomains studied (Fig. 8 b, d). We noted that,
280 areas of overestimation coincide with areas of excessive R1mm values (Fig.2b, d). The
281 strongest overestimation is found over the Guinea Coast, reaching 59.21 and 60.51 days (resp.
282 for JJAS 2003 and JJAS 2004, Table 2).

283 Figure 8 (second panel) is the same as figure 2 (second panel), but displays changes in CWD.
284 As for R1mm index, over the Central Sahel, the dry (wet) experiments decrease (increase) CWD
285 length for both JJAS 2003 and JJAS 2004. This result confirms the strong influence of soil
286 moisture initial conditions in the Sahel band, as found by Zhang et al. (201) and Koster et al.
287 (2006) over the transition zones with a climate between dry and wet regimes. However, over
288 Guinea and the West Sahel, the changes are not linear, both dry and wet experiments increase
289 the CWD length (Fig. 8e-h).

290 Figure 9, as in figure 3, but shows the PDF distribution of changes in CWD. The strongest
291 CWD increase is found over Central Sahel with maximum changes reaching 15.58 days in wet
292 experiments, while the strongest CWD decrease is found in the same sub-domain with
293 maximum changes reaching -4.48 days dry experiments.

294 Summarizing the results of this section, as for R1mm and CDD indices, the impact of wet and
295 dry experiment on CWD is linear over the Central Sahel meaning that dry (wet) experiments
296 decrease (increase) the CWD lengths. The model RegCM4 overestimates the duration of wet
297 consecutive days over most of studied subdomains. This overestimation is associated with the
298 excessive number of wet days in the model as documented by Diaconescu et al. (2014).

299

300 **3.1.5 Maximum one-day precipitation accumulation (RX1day).**

301 The maximum one-day precipitation accumulation (RX1day) during JJAS 2003 and JJAS 2004
302 is assessed in this section. Figure 10 (first panel) shows the spatial distribution of RX1day.
303 CHIRPS observation confines the spatial extent of RX1day maximum values greater than 80
304 mm over the coastline of the Guinea Coast. While, the large extent of RX1day minimum values
305 less than 50 mm are found over the Sahara, Sahel and part of Guinea Coast.

306 The control experiments capture the spatial pattern of RX1day with PCC values around 0.50
307 and 0.4 for JJAS 2003 and JJAS 2004, respectively (Table 2). This low coefficient of PCC is
308 also obtained by Thanh et al. (2017) over Asia with RegCM4 (correlation < 0.3). The model
309 simulations fail to capture the magnitude and spatial extent of the RX1day maxima. The control
310 experiments underestimate the RX1day over most of studied subdomains and this seems to be
311 associated with the excessive number of weak precipitation simulated by the model. The largest
312 underestimation is located over the Guinea Coast and the West Sahel. For instance, over the
313 West Sahel, the MB values are -38.07 and -36.67 mm for JJAS 2003 and JJAS 2004,
314 respectively (Table 2).

315 Figure 10 (second panel) is similar to Figure 2 (second panel), but displays changes in the
316 RX1day. As for the SDII, the impact of the soil moisture initial conditions on RX1day is not
317 linear (Fig. 10, second panel).

318 Figure 11 is similar to figure 3, but shows the PDF distribution of changes in the RX1day.
319 Increases of RX1day for both dry and wet experiments are found over most of studied
320 subdomains (Fig.11). The strongest increase in RX1day is found over Guinea Coast for wet
321 experiments, with values reaching 26.14 and 14.93 during JJAS 2003 and JJAS 2004,
322 respectively (Table 3).

323 In summary, RegCM4 underestimates the maximum one-day precipitation accumulation over
324 most of studied domain. Both wet and dry experiments lead to an increase of RX1day.

325

326 **3.1.6 Precipitation percent due to very heavy precipitation days (R95pTOT)**

327 In this section, we investigated the precipitation percentage due to very heavy precipitation days
328 during JJAS 2003 and JJAS 2004. Figure 12 (first panel) is the same as figure 2 (first panel),
329 but shows the spatial distribution of R95pTOT. CHIRPS observation confines the R95pTOT
330 maximum values greater than 40% over the Guinea Coast. While R95pTOT index minimum
331 values less than 30 % are found over the Central and West Sahel (Fig. 10 a, c). The control
332 experiments (Fig. 12b, d) capture the large spatial pattern with PCC values of 0.59 and 0.55 for
333 JJAS 2003 and JJAS 2004, respectively (Table 2). As with SDII and RX1day indices, the
334 control experiments underestimate the values of the R95pTOT index, while they overestimate
335 the R1mm index. This is also due to the current physical parameterization scheme of the
336 RegCM4 model, which results in a positive bias for the number of wet days with a low
337 precipitation amount (e.g., 1 mm.day⁻¹), and a negative bias in the number of wet days with a
338 higher precipitation threshold (e.g., 10 mm.day⁻¹, not showed here).

339 The control experiments underestimate R95pTOT over the different studied domains. The
340 highest R95pTOT underestimation is found over the Guinea Coast with MB values more than
341 -43.22 and -46.61 % for JJAS 2003 and JJAS 2004, respectively (Table 2).

342 Figure 12 (second panel) is similar to figure 2 (second panel), but displays changes in the
343 R95pTOT index. Both dry and wet experiments lead to R95pTOT index increase over the
344 orographic regions. Therefore, the soil moisture initial conditions, whether dry or wet extreme
345 reinforce occurrence of extreme floods events.

346 Figure 13 is the same as figure 3 but shows the PDF distribution of changes in the R95pTOT.
347 The highest R95pTOT increase is found over the West Sahel and Guinea Coast with maximum
348 change values around 4.03% and 4.33% for JJAS 2003 and JJAS 2004, respectively (Table 3).

349 In summary, RegCM4 underestimates R95pTOT while the soil moisture initial conditions,
350 whether dry or wet, increase the precipitation percent due to very heavy precipitation days. This
351 result is consistent with Liu et al. (2014) work over Asia using RegCM4.

352

353 **3.2. Temperature extreme indices**

354 In this section, using daily maximum and minimum temperatures, we analyzed four extreme
355 temperature indices (Table 1) in RegCM4 simulations over West Africa. All temperature
356 indices are calculated for JJAS 2003 and JJAS 2004. Table 4 summarizes the PCC and MB of
357 all temperature indices for the control experiments with initial soil moisture from ERA20C
358 reanalysis, with respect to CPC-T2m observation, calculated over the subdomains presented in
359 Fig. 1, during the JJAS 2003 and JJAS 2004.

360

361 **3.2.1. Maximum value of daily maximum temperature (TXx)**

362 In this section, we analyzed the TXx, which gives the hottest day's temperature during JJAS
363 2003 and JJAS 2004. Figure 14 (first panel) shows the TXx (in °C) from CPC-T2m observation
364 (Fig. 14a, c) for JJAS 2003 and JJAS 2004 and from the mean control experiments (Fig. 14b,
365 d). The CPC-T2m observation shows that the highest TXx values more than 46 °C are found
366 over the Sahara. The lowest TXx index values less than 32 °C are found over the Guinea Coast
367 (Fig. 14a, d). CPC-T2m observation (Fig. 14a, c) shows the lowest TXx values less than 28 °C
368 along the coastline of the Guinea Coast, while the TXx highest values more than 40 °C are
369 found over Sahara and the northern of Sahel (Fig.14a, c),

370 The control experiments (Fig. 14c, f) reasonably replicate the large-scale patterns of the TXx
371 values with PCCs up to 0.99 (Table 3) over the entire West African domain; however, they
372 exhibit some biases at local scale. The control experiments are closer to the maximum and
373 minimum values displayed in the CPC-T2m observation. The control simulations overestimate
374 the TXx values over the Central and West Sahel, and underestimate them over the Guinea Coast
375 (Table 4). The greatest overestimation is found over the West Sahel with MB values around
376 3.02 and 2.02 °C for JJAS 2003 and JJAS 2004, respectively (Table 4). However, the biases
377 obtained for TXx are much lower than those obtained by Thanh et al. (2017), who used
378 RegCM4 over Asia where they reached 8 °C.

379 Figure 14 (second panel) displays changes in TXx for JJAS 2003 and JJAS 2004 in dry (Fig.
380 14g, i) and wet experiments (Fig. 14h, j) with respect to the control experiments; the dotted area
381 showed significant changes with a statistical significance of 95%. Dry experiments lead to an
382 increase of TXx values, while the wet experiments decrease them.

383 The PDF distributions of TXx changes for JJAS 2003 and JJAS 2004 over (a) the Central Sahel,
384 (b) West Sahel, (c) Guinea Coast, and (d) West Africa derived from dry and wet experiments
385 compared to the control experiments are shown in Fig. 15. Table 5 summarizes the maximum
386 values of changes obtained on the PDF of TXx. The strongest decrease (increase) in the TXx

387 index are found over the Central Sahel with a maximum changes around $-2.57\text{ }^{\circ}\text{C}$ (more than
388 $1.69\text{ }^{\circ}\text{C}$) in wet (dry) experiments in JJAS 2004.

389 In summary, during JJAS 2003 and JJAS 2004, the RegCM4 model overestimates and
390 underestimates the hottest day's temperature over the Sahel and Guinea Coast, respectively.
391 Dry experiments result in an increase of TXx, while the wet experiments lead to a decrease TXx
392 values.

393

394 **3.2.2. Minimum value of daily maximum temperature (TXn).**

395 In this section, we investigated the TXn index which gives the lowest day's temperature during
396 JJAS 2003 and JJAS 2004. Figure 16 (first panel) is the same as figure 14 (first panel) but
397 presents the spatial distribution of the TXn index. CPC-T2m observation displays maxima
398 (greater than 36°C) and minima (less than 24°C) of TXn over the Sahara and the Guinea Coast
399 respectively (Fig.16a, c).

400 The control experiments (Fig.16b, d) show a good agreement with the CPC-T2m datasets in the
401 large scale patterns with PCC of approximately 0.99, however, the magnitude of the TXn index
402 over most of studied domain is overestimated. The strongest positive bias was observed over
403 West Sahel domain with MB about 6.56 and $5.44\text{ }^{\circ}\text{C}$ for JJAS 2003 and JJAS 2004, respectively
404 (Table 4). The TXn biases of our study are lower than those obtained by Thanh et al. (2017) in
405 their work over Asia using RegCM4. As for Fig.14 (second panel), the Figure 16 (second panel)
406 displays changes in TXn index. Dry experiments increase TXn index values while the wet
407 experiments decrease them.

408

409 Figure 16 (second panel) is similar to figure 14 (second panel) but displays the PDF distribution
410 of changes in TXn. The impact on TXn is rather weak compared to the TXx. The strongest
411 increase of TXn index are found over the Central Sahel reaching $1.03\text{ }^{\circ}\text{C}$ in dry experiments
412 during JJAS 2004 (Table 5). While the strongest decrease are found over the West Sahel about
413 -1.67°C for wet experiments during JJAS 2004 (Table 5).

414 In summary, RegCM4 overestimates the lowest day's temperature during JJAS 2003 and JJAS
415 2004 over the whole West African domain. As for TXx index, dry (wet) experiments increase
416 (decrease) the TXn values.

417

418 **3.2.3. Minimum value of daily minimum temperature (TNn index).**

419 In this section, we examined the TNn index, which gives the lowest temperature at night during
420 JJAS 2003 and JJAS 2004. Figure 18 (first panel) is the same as figure 14 (first panel) but
421 displays the spatial distribution of the TNn index. CPC-T2m observations (Fig. 18 a, c) shows
422 TNn maxima with values not exceeding 27 °C, above 15 °N latitude, while the minima values
423 (less than 17 °C) are found over the mountainous regions such as the Cameroon Mountains, Jos
424 Plateau, and Guinea Highlands.

425 The control experiments (Fig. 18 b, d) show good agreement with CPC-T2m observations with
426 PCC of approximately 0.99; however, they exhibit some biases at the local scale. The control
427 experiments overestimate the magnitude of the TNn index over most of studied domains.

428 The strongest positive biases are found over the West Sahel with MB reaching 3.30 °C and 2.55
429 °C for JJAS 2003 and JJAS 2004, respectively (Table 4). These positive biases obtained for the
430 TXx, TXn, and TNn indices are opposite to the cold bias known from RegCM4 in mean climate
431 simulation (Koné et al., 2018, Klutse et al., 2016). It is difficult to determine the origin of
432 RegCM4 temperature biases, as they can depend on several factors, such as surface energy
433 fluxes and water, cloudiness, and surface albedo (Sylla et al., 2012; Tadross et al., 2006).

434 Figure 18 (second panel) is the same as figure 14 (second panel), but displays changes in the
435 TNn. Over the Central and West Sahel, both dry and wet experiments decrease the TNn values.
436 Conversely, over the Guinea Coast, they increase the TNn values.

437 Figure 19 is the same as Figure 15 but shows the PDF distribution of changes in the TNn. Wet
438 (dry) experiments increase (decrease) the TNN values, especially over the Central Sahel. Table
439 5 shows that the strongest increase in TNn index in wet experiments is found over Guinea Coast,
440 with maximum change around 0.11 °C in JJAS 2004, while the strongest decrease in TNn is
441 found in dry experiments over the West Sahel, with maximum change around -1.15 °C in JJAS
442 2003.

443

444 In summary, RegCM4 overestimates the lowest temperature at night during JJAS 2003 and
445 JJAS 2004. Wet (dry) experiments lead to an increase (a decrease) of the TNN index.

446

447 **3.2.4. Maximum value of daily minimum temperature (TNx)**

448 In this section, the index TNx which gives the warmest night temperature during JJAS 2003
449 and JJAS 2004 is analyzed. Figure 20 (first panel) is the same as figure 14 (first panel), but for
450 the TNx index. CPC-T2m observation (Fig. 20a, c) shows the maxima of the TNx index over

451 the Sahara with values reaching 40 °C, while the minima around 24 °C are located over the
452 Guinea Coast.

453 The control experiments (Fig. 20b, d) well reproduced the general features of the TNx index
454 with a PCC value reached 0.99, but some differences exist at local scale. Unlike the TNn index,
455 control experiments underestimate the TNx over most of the studied domain. The strongest
456 negative biases are found over the Central Sahel, with MB values up to -3.35 °C and -3.32 °C
457 for JJAS 2003 and JJAS 2004, respectively (Table 4). The TNx index underestimation seems
458 to be systematically related to the cold bias in RegCM4 over West Africa, which has been
459 reported in several papers (Koné et al., 2018, Klutse et al., 2016).

460 Figure 20 (second panel) is the same as figure 14 (second panel) but displays changes in the
461 TNx. Like for TNn index, over the Central Sahel, dry experiments increase the TNx values,
462 while the wet experiments decrease them. However, over the West Sahel, both wet and dry
463 experiments led to a dominant decrease. Conversely, over the Guinea Coast, although the signal
464 is weak, both dry and wet experiments led to a dominant increase.

465 Figure 21 is the same as figure 15 but displays the PDF distributions of the changes in the TNx.
466 The highest TNx increase (decrease) is found over the Central Sahel in dry (wet) experiments
467 with maximum changes up to 0.25 (-1.67 °C) for JJAS 2003 (JJAS 2004) (Table 5). In
468 summary, RegCM4 underestimates the warmest night temperature and dry (wet) experiments
469 lead to an increase (decrease) of TNx magnitude.

470

471 **4. Conclusions**

472 The impact of the soil moisture initial conditions on six precipitation extreme indices and four
473 temperature extreme indices over West Africa was investigated using the RegCM4-CLM45.
474 We first evaluated the performance of RegCM4-CLM4.5 in representing these climate extreme
475 indices over West Africa. We then performed sensitivity studies over the West African domain,
476 with a spatial resolution of 25 km. We initialized the control runs using ERA20C reanalysis soil
477 moisture and for dry and wet experiments, we used the maximum and minimum values of
478 ERA20C over the whole domain, respectively. Results have been presented for JJAS 2003 and
479 JJAS 2004 which are the two contrasted runs most sensitive to the effects of dry and wet soil
480 moisture initial conditions.

481 Compared to CHIRPS observation, the model overestimates and underestimates the number of
482 wet days. RegCM4 also underestimates the simple daily precipitation intensity index (SDII),

483 the maximum 1-day precipitation (Rx1day), and the precipitation percentage due to very heavy
484 precipitation days (R95pTOT). The current physical parameterization scheme of the RegCM4
485 model used in our study results in a positive bias of the number of wet days with a low
486 precipitation threshold (e. g. 1 mm.day⁻¹), and in a negative bias for a higher precipitation
487 threshold (e.g. 10 mm.day⁻¹, not shown here). RegCM4 generally overestimates the CWD and
488 CDD indices over West Africa. Most of the temperature extreme indices used in this study
489 (TXx, TXn, and TNn) are also overestimated, except the TNx index, which is underestimated
490 over the West Africa domain.

491 The impact on extreme precipitation indices of the soil moisture initial conditions is linear over
492 the Sahel central, only for indices related to the number of precipitation events (R1mm, CDD,
493 and CWD indices) meaning that wet (dry) experiments lead to an increase (decrease) of the
494 number of days, and not for those related to the amount or intensity of precipitation (SDII,
495 RX1day, and R95pTOT). However, the dry and wet experiments increase the precipitation
496 percentage due to very heavy precipitation days and the maximum one-day precipitation
497 accumulation (R95pTOT and RX1day indices, respectively) over most of the studied domain.

498 The soil moisture initial conditions unequally influence the daily maximum and minimum
499 temperatures over the West African domain. The impact on daily maximum temperature
500 extremes are greater than those on the daily minimum temperature extremes. These results are
501 consistent with previous studies (Jaeger and Seneviratne, 2011; Zhang et al., 2009). The wet
502 (dry) experiments lead to TXx and TXn increase (decrease) over West Africa. However,
503 regarding the minimum temperature we showed that dry (wet) experiments lead to a TNx
504 increase (decrease).

505 This study helped to quantify the impact of the soil moisture initial conditions on precipitation
506 and temperature extreme events in terms of intensity, frequency and duration over West Africa.

507 This study is the first to investigate the impact of soil moisture initial conditions on climate
508 extreme indices over West Africa. These experiments were done in a highly-idealized framework
509 and were intended to show the potential impact of very strong soil moisture initial conditions on
510 climate extremes. Consequently, it should be considered as a first overview of the influence of
511 initial soil moisture on climate extremes with a RCM (RegCM4). In perspectives, this study will
512 benefit from being performed in a multi-model framework with several RCMs within
513 CORDEX-Africa initiative (Coordinated Regional Downscaling Experiment).

514 **Author contribution**

515 The authors declare to have no conflict of interest with this work. B. Koné and A. Diedhiou
516 fixed the analysis framework. B. Koné carried out all the simulations and figures production
517 according to the outline proposed by A. Diedhiou. B. Koné and A. Diedhiou, S. Anquetin and
518 A. Diawara worked on the analyses. All authors contributed to the drafting of this manuscript.

519

520 **Acknowledgements**

521 The research leading to this publication is co-funded by the NERC/DFID “Future Climate for
522 Africa” programme under the AMMA-2050 project, grant number NE/M019969/1 and by
523 IRD (Institut de Recherche pour le Développement; France) grant number UMR IGE
524 Imputation 252RA5.

525

526 **References:**

527

528 Bichet, A., & Diedhiou, A. : West African Sahel has become wetter during the last 30 years,
529 but dry spells are shorter and more frequent. *Climate Research*, 75(2), 155-162, (2018a)

530

531 Bichet, A., & Diedhiou, A.: Less frequent and more intense rainfall along the coast of the Gulf
532 of Guinea in West and Central Africa (1981 2014). *Climate Research*, 76(3), 191-201, (2018b)

533

534 **Damien Decremer, Chul E. Chung, Annica M. L. Ekman & Jenny Brandefelt (2014) Which**
535 **significance test performs the best in climate simulations?, *Tellus A: Dynamic Meteorology***
536 **and *Oceanography*, 66:1, DOI: 10.3402/tellusa.v66.23139.**

537

538 Danielson J.J., and Gesch D.B.: Global multi-resolution terrain elevation data 2010
539 (GMTED2010): U.S. Geological Survey Open-File Report 2011–1073, 26 p, 2011.

540

541 Didi Sacré Regis M , Mouhamed, L., Kouakou, K., Adeline, B., Arona, D., Koffi Claude A, K.,
542 ... & Issiaka, S. (2020). Using the CHIRPS Dataset to Investigate Historical Changes in
543 Precipitation Extremes in West Africa. *Climate*, 8(7), 84.

544

545 Diaconescu E. P., Gachon P. , Scinocca J., and LapriseR.: Evaluation of daily precipitation
546 statistics and monsoon onset/retreat over West Sahel in multiple data sets. *Climate Dyn.*, 45,
547 1325–1354, doi:10.1007/s00382-014-2383-2, 2015 .
548

549 Easterling, D.R., Meehl, G.A., Parmesan, C., Changnon, S.A., Karl, T.R. and Mearns, L.O.:
550 Climate Extremes: Observations, Modeling and Impacts. *Science* , 289, 2068-2074.
551 <https://doi.org/10.1126/science.289.5487.2068>, 2000.
552

553 Emanuel K. A.: A scheme for representing cumulus convection in large-scale models. *Journal*
554 *of the Atmospheric Science* 48: 2313–2335, 1991.
555

556 Fan Y., and van den Dool H. : A global monthly land surface air temperature analysis for 1948
557 -present, *J. Geophys. Res.* 113, D01103, doi: 10.1029/2007JD008470, 2008.
558

559 Folland C. K., Palmer T. N. , and Parker D. E.: Sahel rainfall and worldwide sea
560 temperatures, *Nature*, 320, 602 – 607, 1986.
561

562 Fontaine B., Janicot S. , and Moron V. : Rainfall anomaly patterns and wind field signals over
563 West Africa in August (1958 – 1989), *J. Clim.*, 8, 1503 –1510, 1995.
564

565 Giorgi F., Coppola E., Solmon F., Mariotti L., Sylla M. B., Bi X., Elguindi N., Diro G. T., Nair
566 V., Giuliani G., Cozzini S., Guettler I., O’Brien T., Tawfik A., Shalaby A., Zakey A. S., Steiner
567 A., Stordal F., Sloan L., and Brankovic C. : RegCM4: model description and preliminary tests
568 over multiple CORDEX domains, *Clim. Res.*, 52, 7–29, doi.org/10.3354/cr01018, 2012.
569

570 Grell G., Dudhia J. and Stauffer D. R.: A description of the fifth generation Penn State/NCAR
571 Mesoscale Model (MM5), National Center for Atmospheric Research Tech Note NCAR/TN-
572 398+STR, NCAR, Boulder, CO, 1994.
573

574 Holtslag A., De Bruijn E., and Pan H. L. : A high resolution air mass transformation model for
575 short-range weather forecasting, *Mon. Weather Rev.*, 118, 1561–1575, 1990.
576

577 Hong S. Y. and Pan H. L.: Impact of soil moisture anomalies on seasonal, summertime
578 circulation over North America in a regional climate model. *J. Geophys. Res.*, 105 (D24), 29
579 625–29 634, 2000.

580

581 Jaeger E. B., and Seneviratne S. I. : Impact of soil moisture-atmosphere coupling on
582 European climate extremes and trends in a regional climate model, *Clim. Dyn.*, 36(9-10),
583 1919-1939, doi:10.1007/s00382-010-0780-8, 2011.

584

585 Kang S, Im E.-S. and Ahn J.-B.: The impact of two land-surface schemes on the characteristics
586 of summer precipitation over East Asia from the RegCM4 simulations *Int. J. Climatol.* 34:
587 3986–3997, 2014.

588

589 Kim J-E., and Hong S-Y.: Impact of Soil Moisture Anomalies on Summer Rainfall over East
590 Asia: A Regional Climate Model Study, *Journal of Climate*. Vol. 20, 5732–5743, DOI:
591 10.1175/2006JCLI1358.1, 2006.

592

593 Kiehl J. T., Hack J. J., Bonan G. B., Boville, B. A., Briegleb B. P., Williamson D. L., and Rasch
594 P. J.: Description of the NCAR Community Climate Model (CCM3), Technical Note
595 NCAR/TN–420+STR, 152, 1996.

596

597 Koné B., Diedhiou A., N’datchoh E. T., Sylla M. B. , Giorgi F., Anquetin S., Bamba A.,
598 Diawara A., and Koba A. T.: Sensitivity study of the regional climate model RegCM4 to
599 different convective schemes over West Africa. *Earth Syst. Dynam.*, 9, 1261–1278.
600 <https://doi.org/10.5194/esd-9-1261-2018>, 2018.

601

602

603 Koster R. D., GUO Z. H., Dirmeyer P. A., Bonan G., Chan E., Cox P., Davies H., Gordon C.
604 T., Gordon C. T., Lawrence D., Liu P., Lu C. H, Malyshev S., McAvaney B., Mitchell K, Mocko
605 D., Oki K., Oleson K., Pitman A., Sud Y. C. , Taylor C. M., 16 Versegby D., Vasic R., Xue
606 Y., Yamada T.: The global land–atmosphere coupling experiment. Part I: Overview, *J.*
607 *Hydrometeorol.*, 7(4), 590–610, doi:10.1175/JHM510.1, 2006.

608

609 Larsen J.: Record heat wave in Europe takes 35,000 lives. Earth Policy Institute, 2003.
610

611 Le Barbé L., Lebel L., and Tapsoba D.: Rainfall variability in west africa during the years 1950-
612 1990. *J. Climate*, 15 :187–202., 2002.

613

614 Loveland TR, Reed BC, Brown JF, Ohlen DO, Zhu Z, Yang L, J. W. Merchant J. W.:
615 Development of a global land cover characteristics database and IGBP DISCover from 1km
616 AVHRR data. *International Journal of Remote Sensing* 21: 1303–1330, 2000.

617

618 Liu D., G. Wang R. Mei Z. Yu, and Yu M. : Impact of initial soil moisture anomalies on climate
619 mean and extremes over Asia, *J. Geophys. Res. Atmos.*, 119, 529–545,
620 doi:10.1002/2013JD020890, 2014.

621

622 Klutse B. A. N., Sylla B. M., Diallo I., Sarr A., Dosio A.,Diedhiou A., Kamga A., Lamptey B.,
623 Ali A., Gbobaniyi E. O., Owusu K., Lennard C., Hewitson B., Nikulin G.,& Panitz H.-J.,
624 Büchner M.: Daily characteristics of West African summer monsoon precipitation in CORDEX
625 simulations. *Theor Appl Climatol.* 123:369–386 DOI 10.1007/s00704-014-1352-3, 2016.

626

627 Menéndez, C. G., Giles, J., Ruscica, R., Zaninelli, P., Coronato, T., Falco, M., ... & Li, L.
628 (2019). Temperature variability and soil–atmosphere interaction in South America simulated
629 by two regional climate models. *Climate Dynamics*, 53(5), 2919-2930.

630

631 Nicholson, SE.: The nature of rainfall fluctuations in subtropical West-Africa. *Mon. Wea. Rev.*
632 22109, 2191-2208, 1980.

633

634 Nicholson SE.: Land Surface processes and Sahel climate. *Reviews of Geophysics.* 38(1), 117-
635 24139, 2000.

636

637 Nikulin G., Jones C., Samuelsson P., Giorgi F., Asrar G., Büchner M., Cerezo-Mota R.,
638 Christensen O. B., Déque M., Fernandez J., Hansler A., van Meijgaard E., Sylla M. B. and
639 Sushama L.: Precipitation climatology in an ensemble of CORDEX-Africa regional climate
640 simulations, *J. Climate*, 6057–6078, <https://doi.org/10.1175/JCLI-D-11-00375.1>, 2012.

641
642 Oleson K., Lawrence D. M., Bonan G. B., Drewniak B., Huang M., Koven C. D., Yang Z.-L.:
643 Technical description of version 4.5 of the Community Land Model (CLM) (No. NCAR/TN-
644 503+STR). doi:10.5065/D6RR1W7M, 2013.

645
646 Pal J. S., Small E. E. and Elthair E. A.: Simulation of regional scale water and energy budgets:
647 representation of subgrid cloud and precipitation processes within RegCM, *J. Geophys. Res.*,
648 105, 29579–29594, 2000.

649
650 Pan, Y.; Wang, W.; Shi, W. Assessment of CPC-T2m Global Daily Surface Air Temperature
651 (CPC-T2m) Analysis. *Assessment 2019*, 22, 24.

652
653 Peterson T. C., Folland C., Gruza G., Hogg W. Mokssit A., Plummer N. : Report on the
654 activities of the working group on climate change detection and related rapporteurs 1998-2001.
655 Geneva (Switzerland): WMO Rep. WCDMP 47, WMO-TD 1071, 2001.

656
657 Philippon N., Mouglin E. , Jarlan L. , and Frison P.-L.: Analysis of the linkages between
658 rainfall and land surface conditions in the West African monsoon through CMAP, ERS-
659 WSC, and NOAA-AVHR R data. *J. Geophys. Res.*, 110, D24115,
660 doi:10.1029/2005JD006394, 2005.

661
662 Reynolds, R. W. and Smith, T. M.: Improved global sea surface temperature analysis using
663 optimum interpolation, *J. Climate*, 7, 929–948, 1994.

664
665 Simmons A. S., Uppala D. D. and Kobayashi S.: ERA-interim: new ECMWF reanalysis
666 products from 1989 onwards, *ECMWF Newsl.*, 110, 29–35, 2007.

667 Solmon F., Giorgi F., and Lioussse C.: Aerosol modeling for regional climate studies:
668 application to anthropogenic particles and evaluation over a European/African domain, *Tellus*
669 *B*, 58, 51–72, 2006.

670

671 Sundqvist H. E., Berge E., and Kristjansson J. E.: The effects of domain choice on summer
672 precipitation simulation and sensitivity in a regional climate model, *J. Climate*, 11, 2698–2712,
673 1989.

674

675 Sylla MB, Giorgi F, Stordal F.: Large-scale origins of rainfall and temperature bias in high
676 resolution simulations over Southern Africa. *Climate Res.* 52: 193–211, DOI: 10.3354/cr01044,
677 2012.

678

679 Tadross MA, Gutowski WJ Jr, Hewitson BC, Jack C, New M.: MM5 simulations of interannual
680 change and the diurnal cycle of southern African regional climate. *Theor. Appl. Climatol.* 86(1–
681 4):63–80, 2006.

682

683 Takahashi, H. G., & Polcher, J. (2019). Weakening of rainfall intensity on wet soils over the
684 wet Asian monsoon region using a high-resolution regional climate model. *Progress in Earth
685 and Planetary Science*, 6(1), 1-18.

686

687 Thanh N.-D., Fredolin T. T., Jerasorn S., Faye C., Long T.-T., Thanh N.-X., Tan P.-V., Liew
688 J., Gemma N., Patama S., Dodo G. and Edvin A.: Performance evaluation of RegCM4 in
689 simulating extreme rainfall and temperature indices over the CORDEX-Southeast Asia region.
690 *Int. J. Climatol.* 37: 1634–1647. Published online 28 June 2016 in Wiley Online Library
691 (wileyonlinelibrary.com) DOI: 10.1002/joc.4803, 2017.

692

693 Uppala S., Dee D., Kobayashi S., Berrisford P. and Simmons A.: Towards a climate data
694 assimilation system: status update of ERA-interim, *ECMWF Newsl.*, 15, 12–18, 2008.

695

696 Wang, G., Yu, M., Pal, J. S., Mei, R., Bonan, G. B., Levis, S., and Thornton, P. E.: On the
697 development of a coupled regional climate vegetation model RCM-CLM-CN-DV and its
698 validation its tropical Africa, *Clim. Dynam*, 46, 515–539, 2016.

699

700 You Q., Kang S., Aguilar E., Pepin N., Flügel W.-A., Yan Y. , Xu Y., Zhang Y. , and Huang
701 J. : Changes in daily climate extremes in China and their connection to the large scale
702 atmospheric circulation during 1961–2003, *Clim. Dyn.*, 36(11-12), 2399–2417,
703 doi:10.1007/s00382-009-0735-0, 2010.

704
705 Zakey A. S., Solmon F., and Giorgi F.: Implementation and testing of a desert dust module in
706 a regional climate model, *Atmos. Chem. Phys.*, 6, 4687–4704, [https://doi.org/10.5194/acp-6-](https://doi.org/10.5194/acp-6-4687-2006)
707 4687-2006, 2006.

708
709 Zeng X., Zhao M. and Dickinson R .E.: Intercomparison of bulk aerodynamic algorithms for
710 the computation of sea surface fluxes using TOGA COARE and TAO DATA, *J. Climate*, 11,
711 2628-2644, 1998.

712
713 Zhang J, Wang W.C., and Wu L.: Land–atmosphere coupling and diurnal temperature range
714 over the contiguous United States. *Geophys Res Lett* 36:L06706. doi:10.1029/2009GL037505,
715 2009.

716
717 Zhang J. Y., Wu L. Y. and Dong W.: Land-atmosphere coupling and summer climate
718 variability over East Asia, *J. Geophys. Res.*, 116,D05117, doi 10.1029/2010JD014714, 2011.

719
720
721
722
723
724
725
726
727
728
729
730

731 **TABLES AND FIGURES.**

732

Extreme indices	Definition	Units
-----------------	------------	-------

Extreme Rainfall Indices			
1	R1mm	Number of wet days (daily precipitation ≥ 1 mm)	day
2	SDII	The amount of precipitation mean on wet days (daily precipitation ≥ 1 mm)	mm.day ⁻¹
3	CDD	Maximum number of consecutive dry days (daily precipitation < 1 mm.day ⁻¹)	day
4	CWD	Maximum number of consecutive wet days (daily precipitation ≥ 1 mm.day ⁻¹)	day
5	RX1day	The maximum one-day precipitation accumulation	mm
6	R95pTOT	Precipitation percent due to very heavy precipitation days.	%
Extreme temperature indices			
7	TXn	Minimum value of daily maximum temperature	°C
8	TXx	Maximum value of daily maximum temperature	°C
9	TNn	Minimum value of daily minimum temperature	°C
10	TNx	Maximum value of daily minimum temperature	°C

733

734 **Table1:** The 10 extreme climate indices used in this study.

735

736

737

738

739

Central Sahel		West Sahel		Guinea Coast		West Africa	
MB	PCC	MB	PCC	MB	PCC	MB	PCC

R1mm	CTRL_2003	33.17	0.98	-5.25	0.96	53.16	0.96	22.18	0.96
	CTRL_2004	29.50	0.98	1.34	0.96	55.46	0.96	23.85	0.95
SDII	CTRL_2003	-7.52	0.97	-9.95	0.94	-13.62	0.77	-7.67	0.73
	CTRL_2004	-7.01	0.97	-9.37	0.94	-14.65	0.81	-7.59	0.77
CDD	CTRL_2003	0.93	0.90	14.49	0.91	-7.84	0.66	2.63	0.85
	CTRL_2004	4.75	0.91	17.51	0.95	-9.43	0.68	6.99	0.89
CWD	CTRL_2003	45.56	0.83	18.44	0.75	59.21	0.88	31.20	0.81
	CTRL_2004	36.78	0.79	20.48	0.78	60.51	0.82	29.74	0.79
RX1day	CTRL_2003	-26.46	0.78	-38.07	0.91	-30.28	0.54	-20.08	0.50
	CTRL_2004	-22.89	0.46	-36.67	0.88	-42.44	0.42	-20.23	0.40
R95pTOT	CTRL_2003	-27.67	0.67	-33.39	0.77	-43.22	0.65	-29.12	0.59
	CTRL_2004	-24.38	0.46	-31.75	0.80	-46.61	0.60	-27.45	0.55

740

741 **Table 2:** The pattern correlation coefficient (PCC) and the mean bias (MB) of R1mm (in day),
742 SDII (in mm.day-1), CDD (in day), CWD (in day), RX1day (in mm) and R95pTOT (in %)
743 indices for control experiments (initialized with initial soil moisture of ERA20C reanalysis)
744 with respect to CHIRPS, calculated over Guinea Coast, Central Sahel, West Sahel and the entire
745 West African domain for JJAS 2003 and JJAS 2004.

746

747

748

749

750

Precipitation indices		Central Sahel		West Sahel		Guinea Coast		West Africa	
		ΔWC	ΔDC	ΔWC	ΔDC	ΔWC	ΔDC	ΔWC	ΔDC
R1mm (day)	2003	8.14	-5.19	12.02	0.69	3.92	2.88	4.67	1.75

	2004	10.01	-3.79	10.14	0.56	4.90	3.57	7.90	2.61
SDII (mm/day)	2003	0.07	0.11	-0.11	0.14	0.70	0.17	0.29	0.31
	2004	0.03	0.09	0.26	-0.07	0.56	0.22	0.24	0.21
CWD (day)	2003	13.25	-3.15	6.61	0.64	12.24	4.05	9.43	1.09
	2004	15.58	-4.48	7.20	-0.19	6.08	3.18	11.89	-0.37
CDD (day)	2003	-2.80	2.58	-12.73	0.83	-0.68	-1.31	-1.53	0.19
	2004	-5.92	3.80	-7.75	2.75	-0.93	-1.46	-3.57	-0.44
RX1day (mm)	2003	1.97	3.78	0.11	0.65	26.14	4.17	7.16	7.27
	2004	3.35	3.03	7.05	0.19	14.93	15.73	6.46	2.28
R95pTOT (%)	2003	1.54	1.77	2.88	1.53	4.33	2.37	2.83	2.46
	2004	1.66	0.89	4.03	0.43	1.69	0.92	1.37	2.43

751

752 **Table 3:** Summary Table of maximum values of change on PDF's for R1mm, SDII, CDD,
753 CWD, RX-1day and R95pTOT indices.

754

755

756

757

758

759

760

761

762

763

764

765

766

Central Sahel		West Sahel		guinea		West Africa	
MB	PCC	MB	PCC	MB	PCC	MB	PCC

TXx	CTRL_2003	2.10	0.99	3.02	0.99	-1.34	0.99	0.32	0.99
	CTRL_2004	1.14	0.99	2.02	0.99	-1.41	0.99	-0.16	0.99
TXn	CTRL_2003	5.12	0.99	6.56	0.99	3.76	0.99	5.65	0.99
	CTRL_2004	3.43	0.99	5.44	0.99	2.75	0.99	4.14	0.99
TNn	CTRL_2003	2.37	0.99	3.30	0.99	1.53	0.99	1.45	0.99
	CTRL_2004	2.09	0.99	2.55	0.99	1.28	0.99	0.71	0.99
TNx	CTRL_2003	-1.91	0.99	-2.86	0.99	-3.35	0.99	-3.85	0.99
	CTRL_2004	-1.90	0.99	-2.54	0.99	-3.32	0.99	-3.99	0.99

767

768 **Table 4:** The pattern correlation coefficient (PCC) and the mean bias (MB in°C) of TXx,
769 TXn, TNn and TNx indices for control experiments (initialized with initial soil moisture of
770 ERA20C reanalysis) with respect to CPC-T2m, calculated for Guinea Coast, Central Sahel,
771 West Sahel and the entire West African domain for JJAS 2003 and JJAS 2004.

772

773

774

775

776

777

778

779

780

Temperature	Central Sahel	West Sahel	Guinea Coast	West Africa
-------------	---------------	------------	--------------	-------------

indices		ΔWC	ΔDC	ΔWC	ΔDC	ΔWC	ΔDC	ΔWC	ΔDC
TXx	2003	-2.54	1.14	-2.11	0.90	-0.34	0.68	-0.89	1.06
	2004	-2.57	1.69	-1.58	0.98	-0.32	1.01	-0.86	1.27
TXn	2003	-1.37	0.81	-1.67	-0.05	-0.06	0.28	-0.50	0.59
	2004	-1.09	1.03	-0.93	0.55	-0.04	0.31	-0.38	0.61
TNn	2003	-0.37	-0.20	-0.23	-1.15	0.05	0.04	-0.20	0.03
	2004	-0.03	-0.37	0.06	-1.07	0.11	-0.03	-0.05	-0.11
TNx	2003	-1.29	0.25	-0.94	-1.37	0.12	0.04	-0.49	0.13
	2004	-1.67	0.15	-0.62	-1.13	0.02	0.03	-0.51	-0.07

781

782 **Table 5:** Summary Table of maximum values of change on PDF's for TXx, TXn, TNn and
783 TNx indices.

784

785

786

787

788

789

790

791

792

793

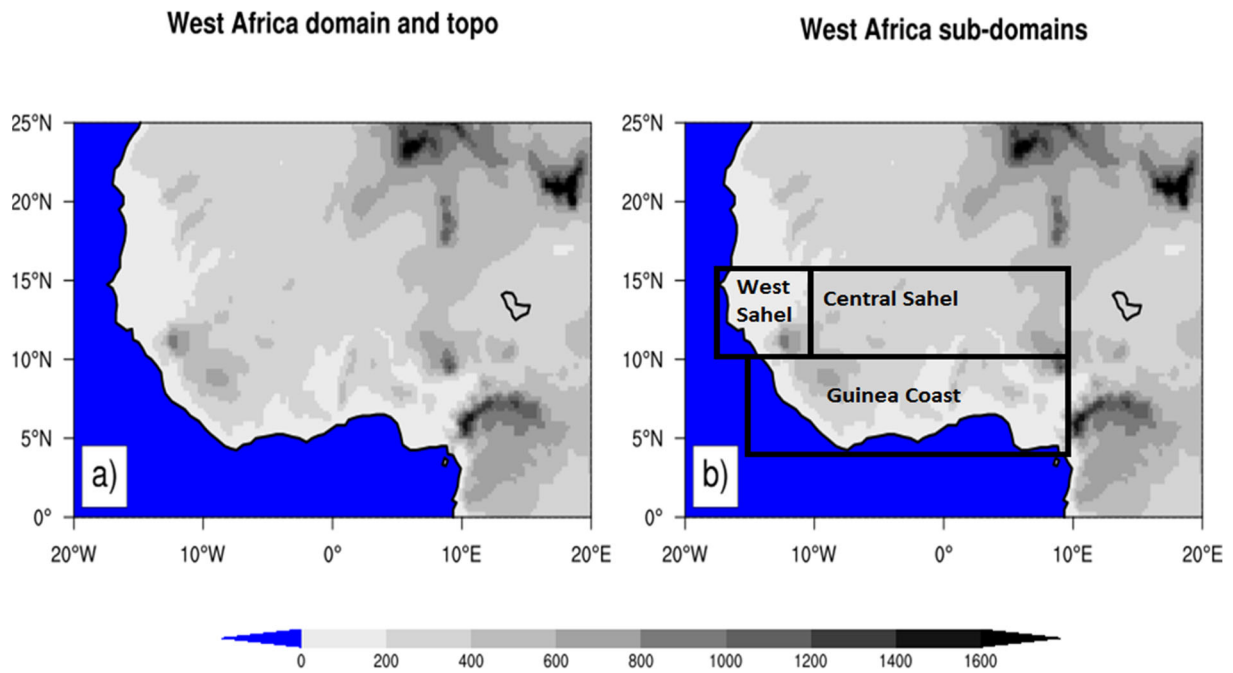
794

795

796

797

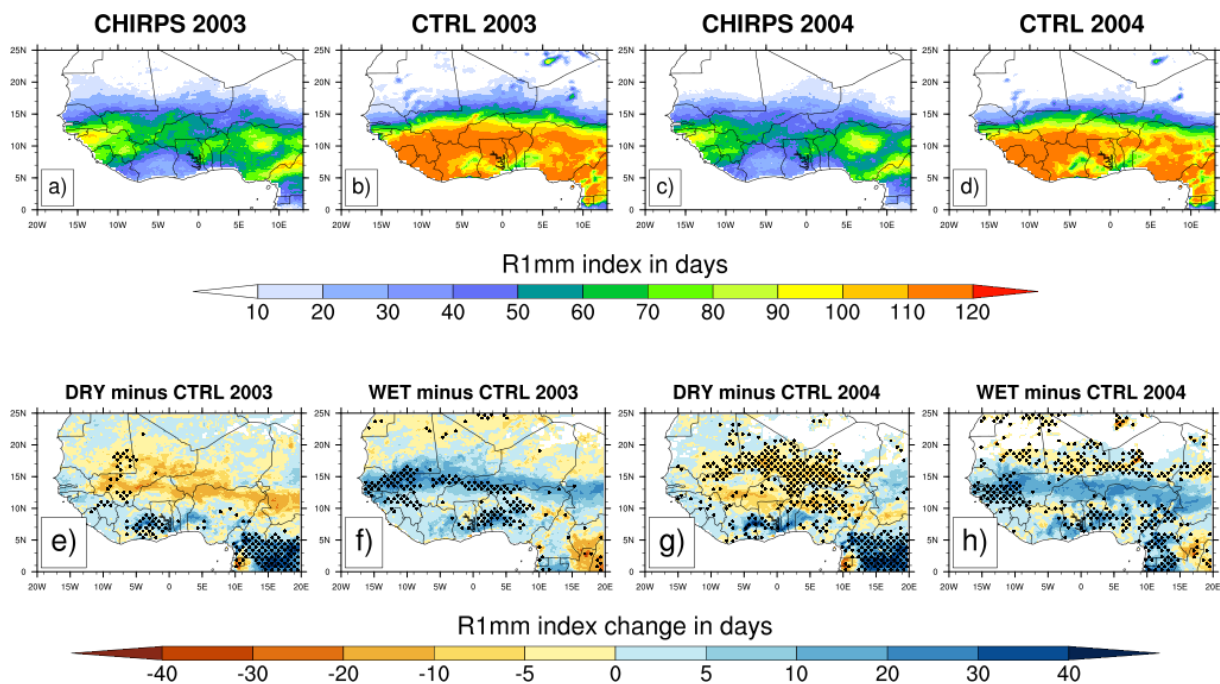
798



799
800

801 **Figure 1:** Topography of the West African domain. The analysis of the model result has an
802 emphasis on the whole West African domain and the three subregions Guinea Coast, Central
803 Sahel and West Sahel, which are marked with black boxes.

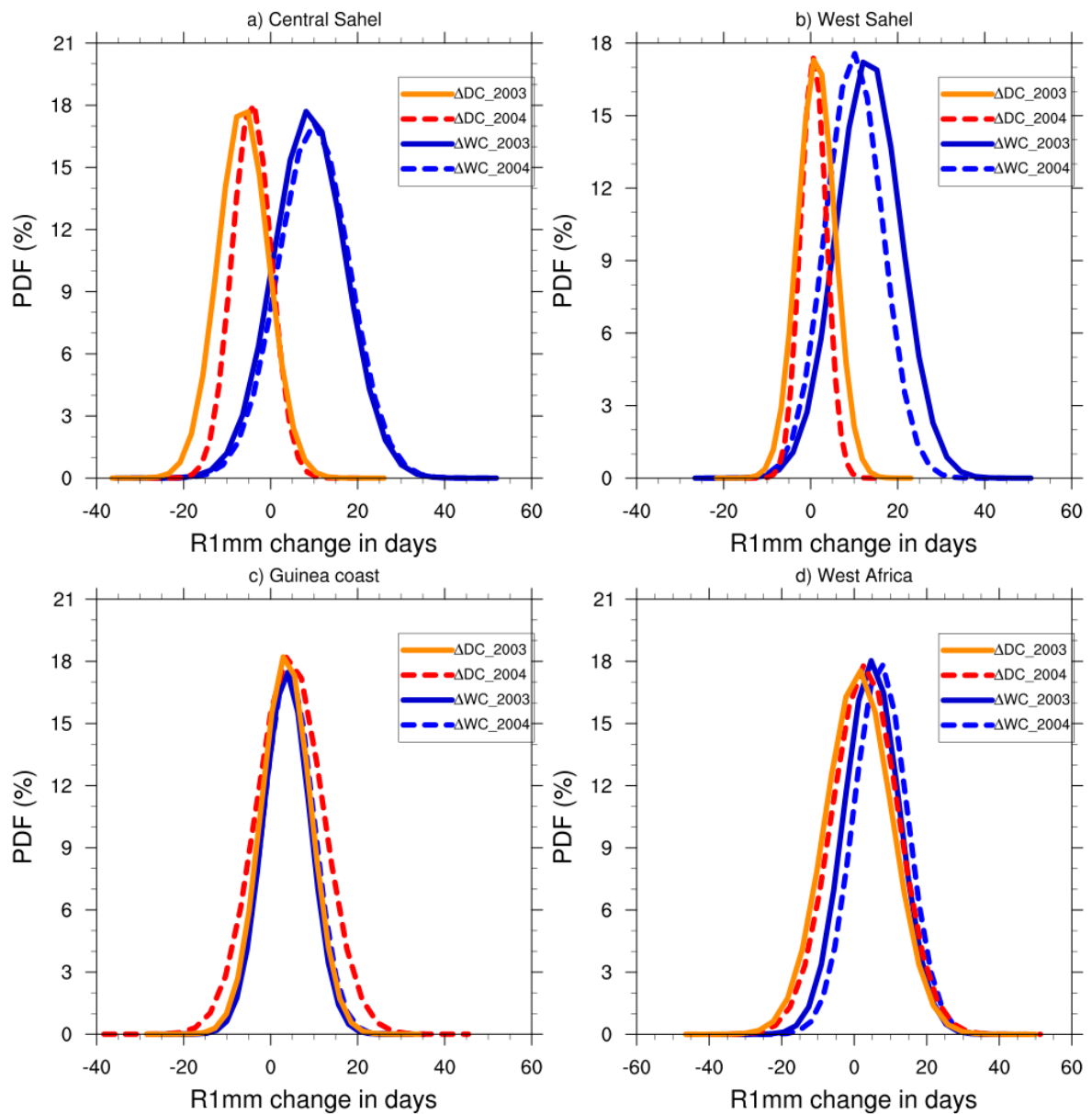
804
805
806
807
808
809
810
811
812
813
814
815
816
817
818
819
820



821
822

823 **Figure2:** Mean values of the number of the wet days (R1mm index in days) from CHIRPS (a
824 and c) observation for JJAS 2003 and JJAS 2004 and the simulated control (CTRL) experiments
825 (b and d) initialized with initial soil moisture of the reanalysis of ERA20C (first panel) and
826 changes in R1mm index in days (second panel) for JJAS 2003 and JJAS 2004, from dry (e and
827 g) and wet (f and h) experiments with respect to the control experiments. Areas with values
828 passing the 95% significance test are dotted.

829
830
831
832
833
834
835
836
837
838
839



840

841

842 **Figure3:** PDF distributions (%) of mean values of the number of the wet days change in JJAS

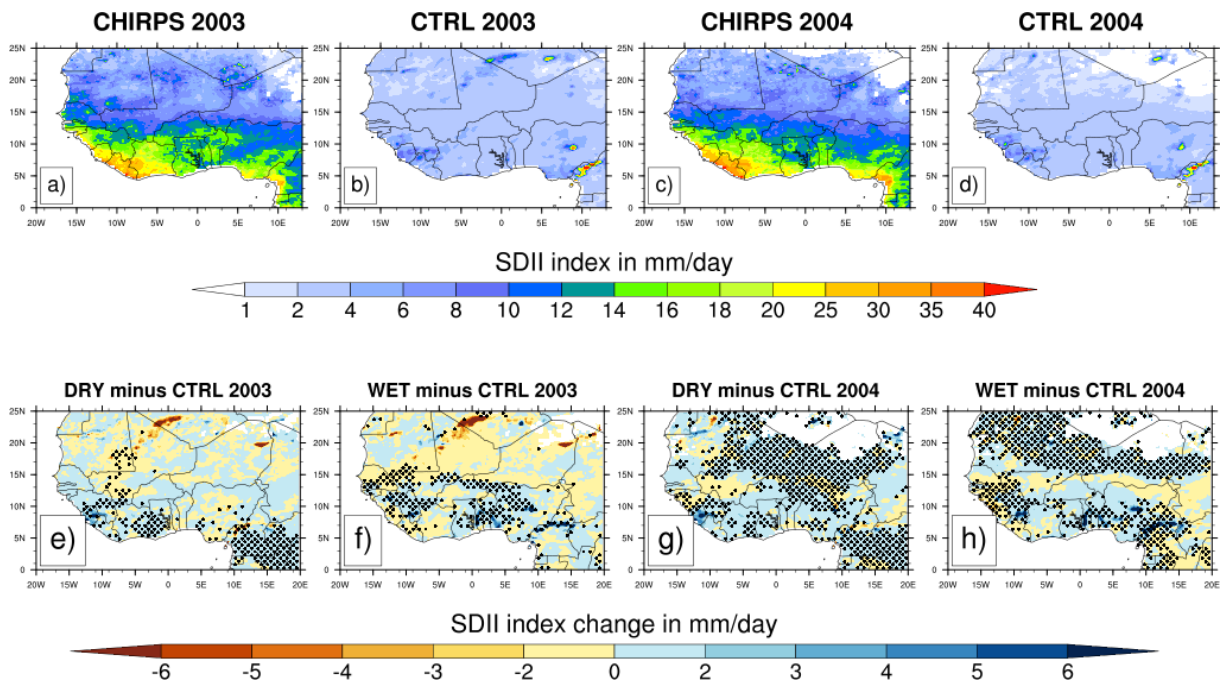
843 2003 and JJAS 2004, over (a) Central Sahel , (b) West Sahel, (c) Guinea and (d) West Africa

844 derived from dry (ΔDC) and wet (ΔWC) experiments with respect to the control experiment.

845

846

847



848

849

850 **Figure4:** Same as Fig. 2 but for the SDII index (in mm.day⁻¹).

851

852

853

854

855

856

857

858

859

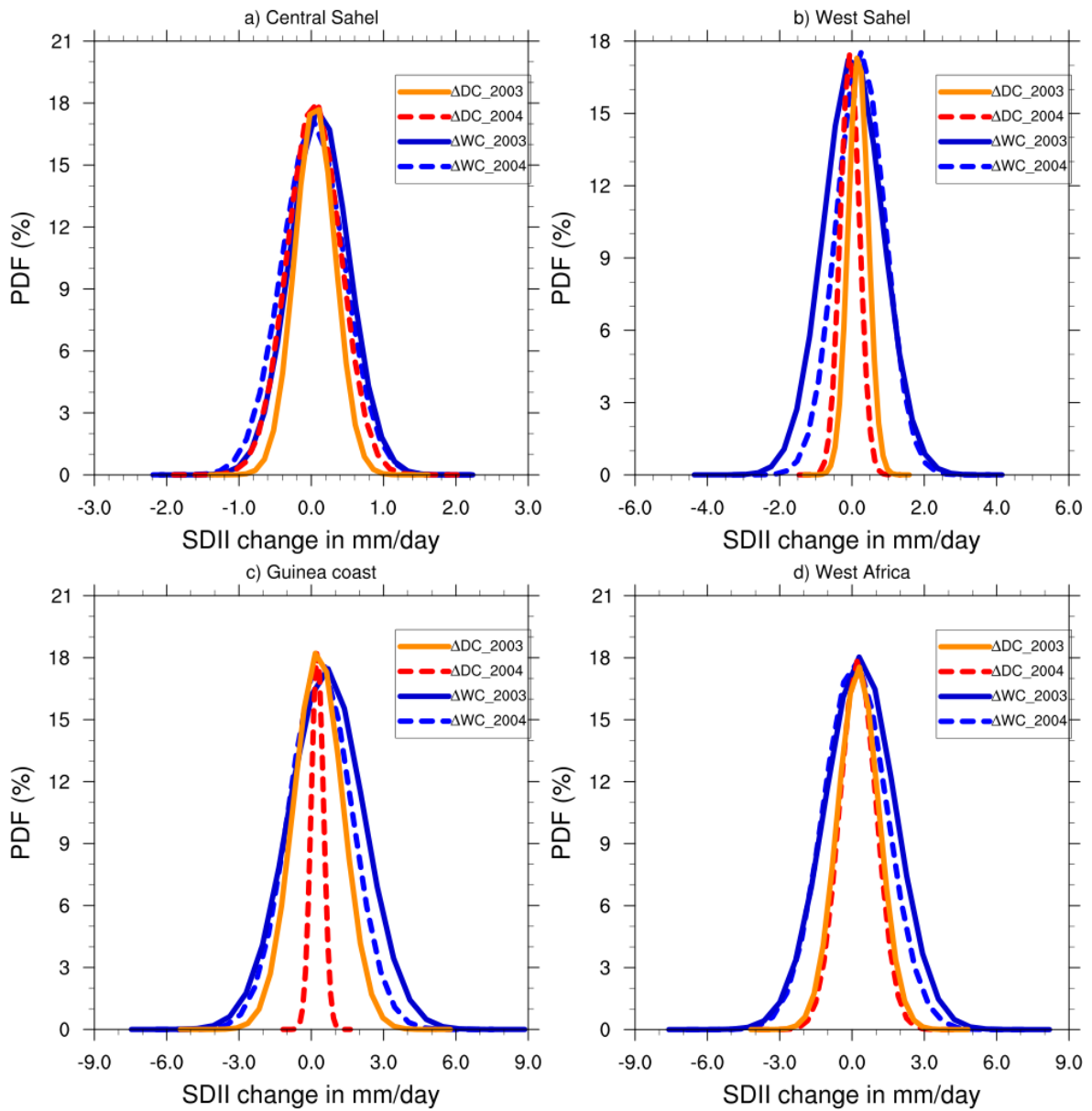
860

861

862

863

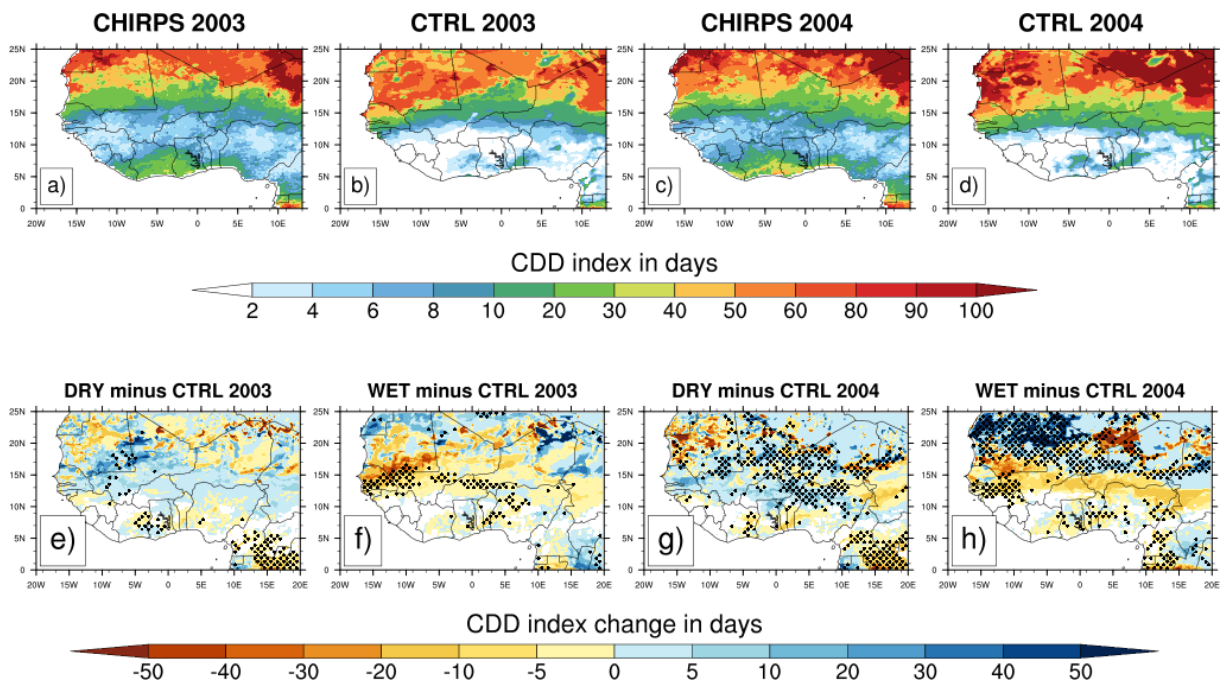
864



865
 866
 867
 868
 869
 870
 871
 872
 873
 874
 875
 876

Figure 5: Same as Fig. 3 but for the SDII index (in mm.day⁻¹).

877



878

879

880 **Figure 6:** Same as Fig. 2 but for the CDD index (in day).

881

882

883

884

885

886

887

888

889

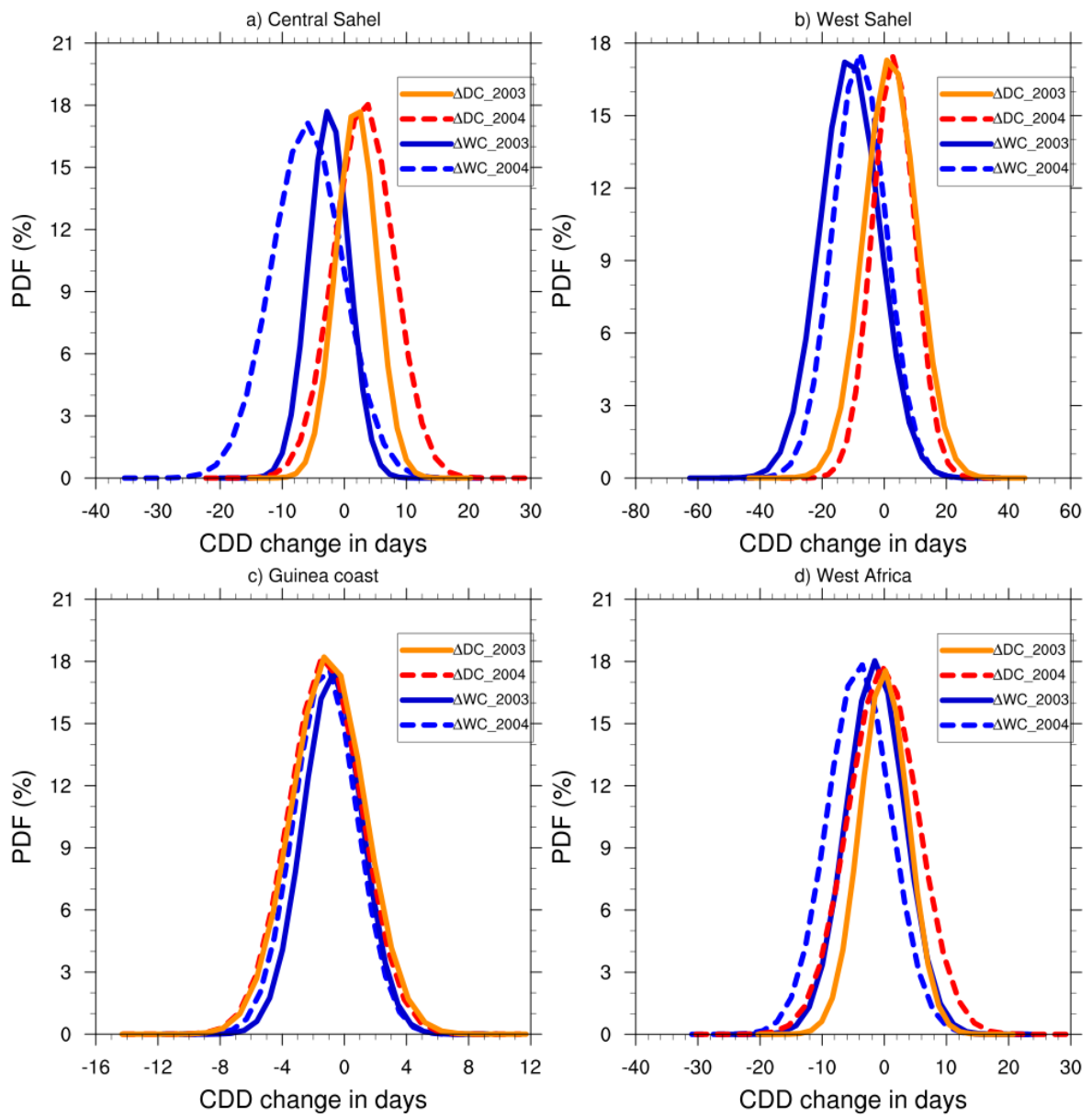
890

891

892

893

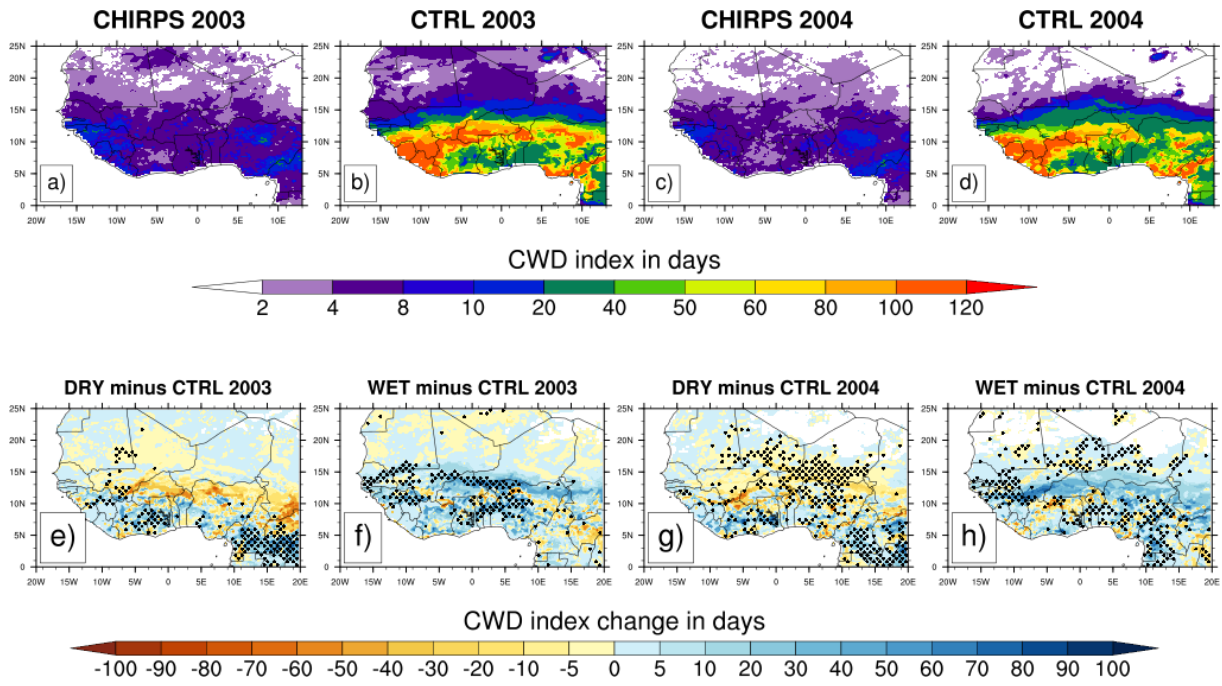
894



895
 896
 897
 898
 899
 900
 901
 902
 903
 904
 905

Figure 7: Same as Fig. 3 but for the CDD index (in day).

906



907

908

909 **Figure 8:** Same as Fig. 2 but for the CWD index (in day).

910

911

912

913

914

915

916

917

918

919

920

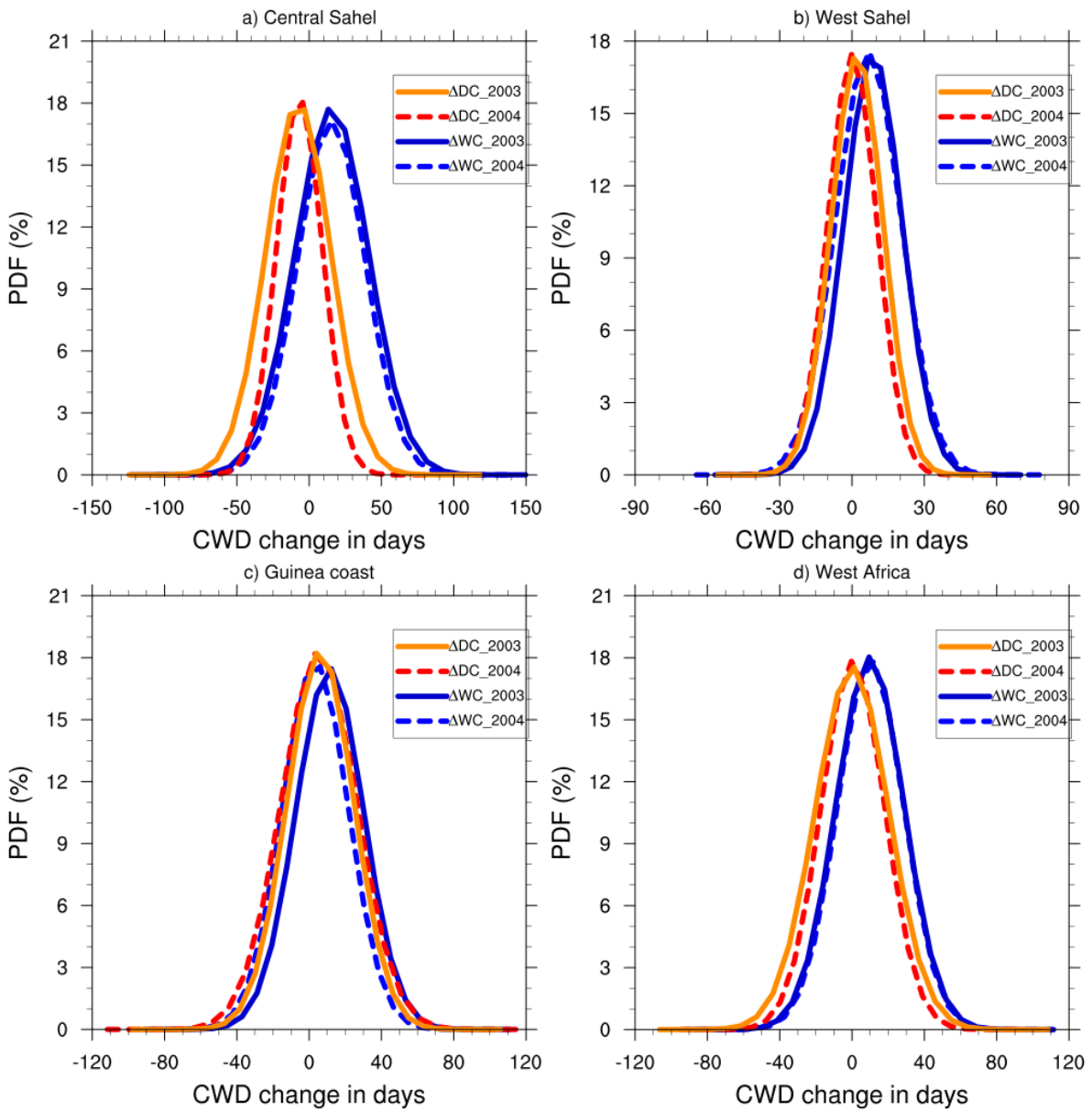
921

922

923

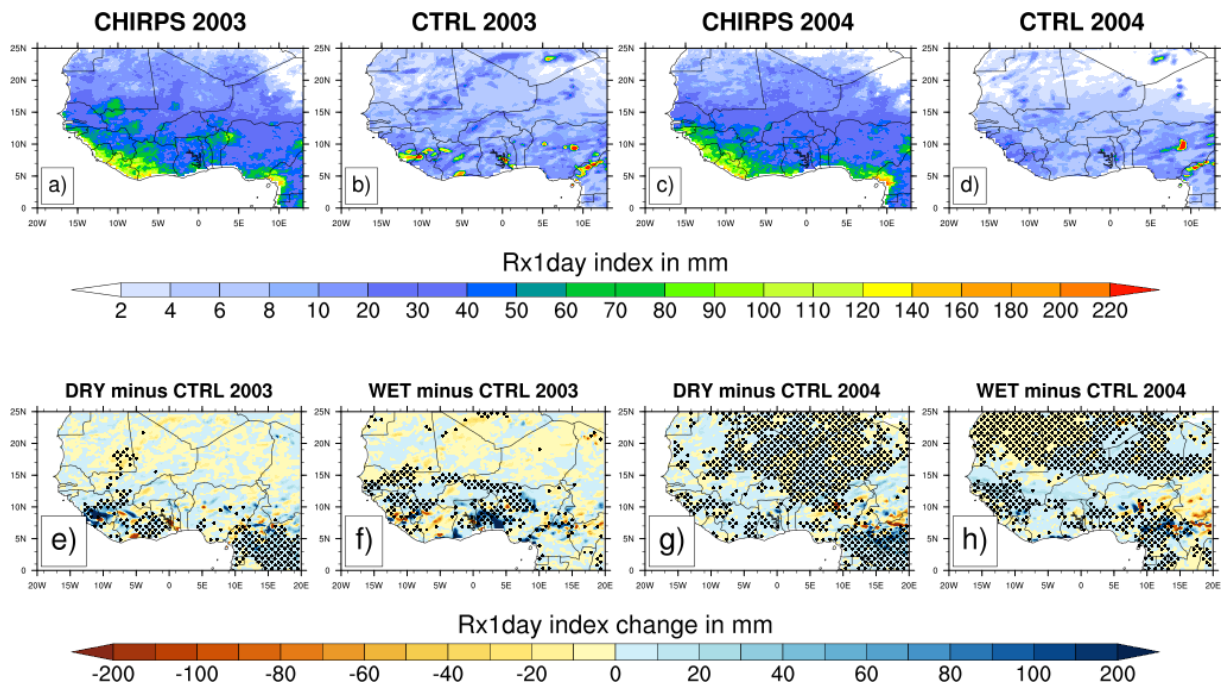
924

925



926
 927
 928
 929
 930
 931
 932
 933
 934
 935
 936
 937

Figure 9: Same as Fig. 3 but for the CWD index (in day).



938

939

940 **Figure 10:** Same as Fig. 2 but for the RX1day index (in mm).

941

942

943

944

945

946

947

948

949

950

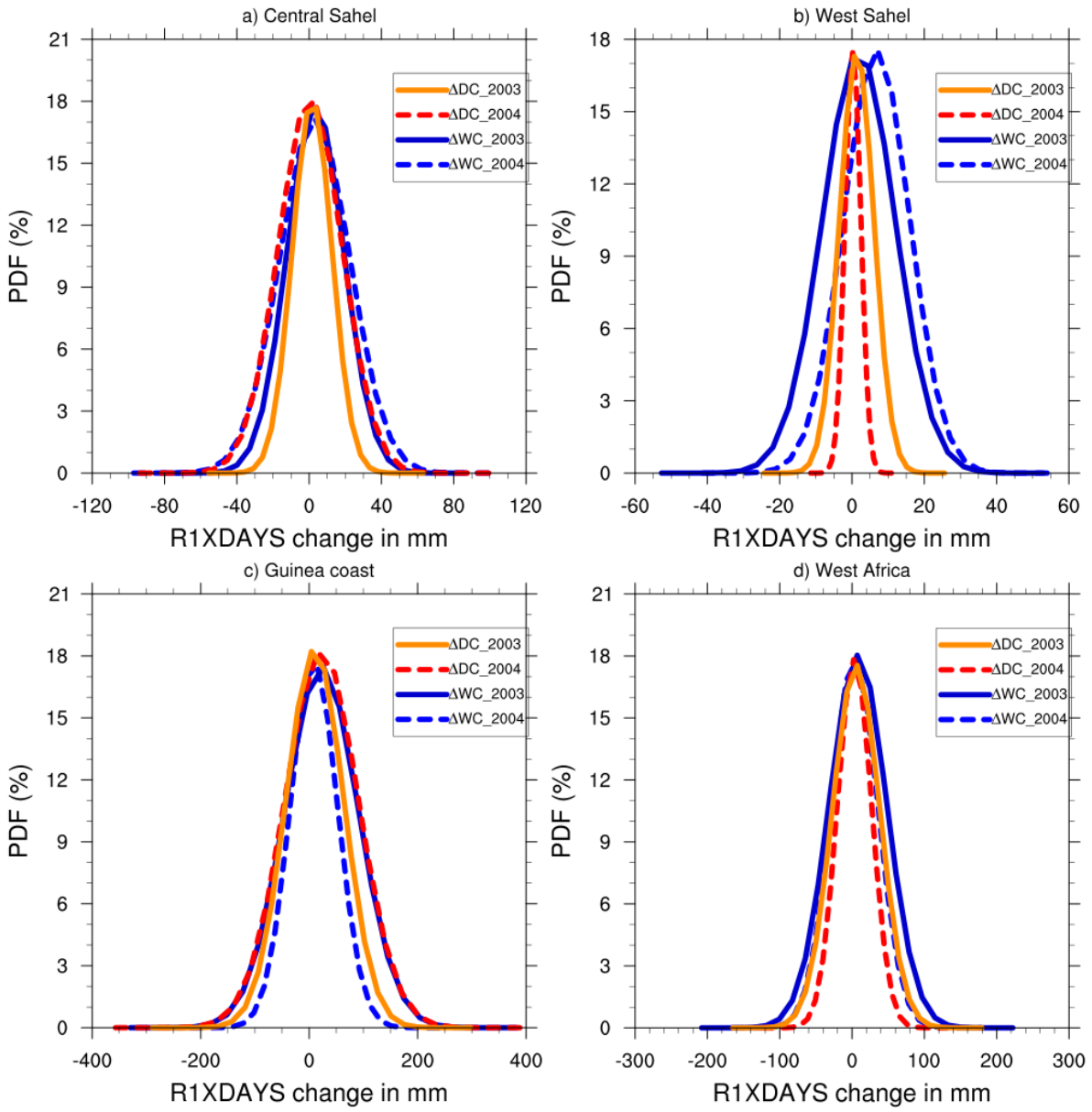
951

952

953

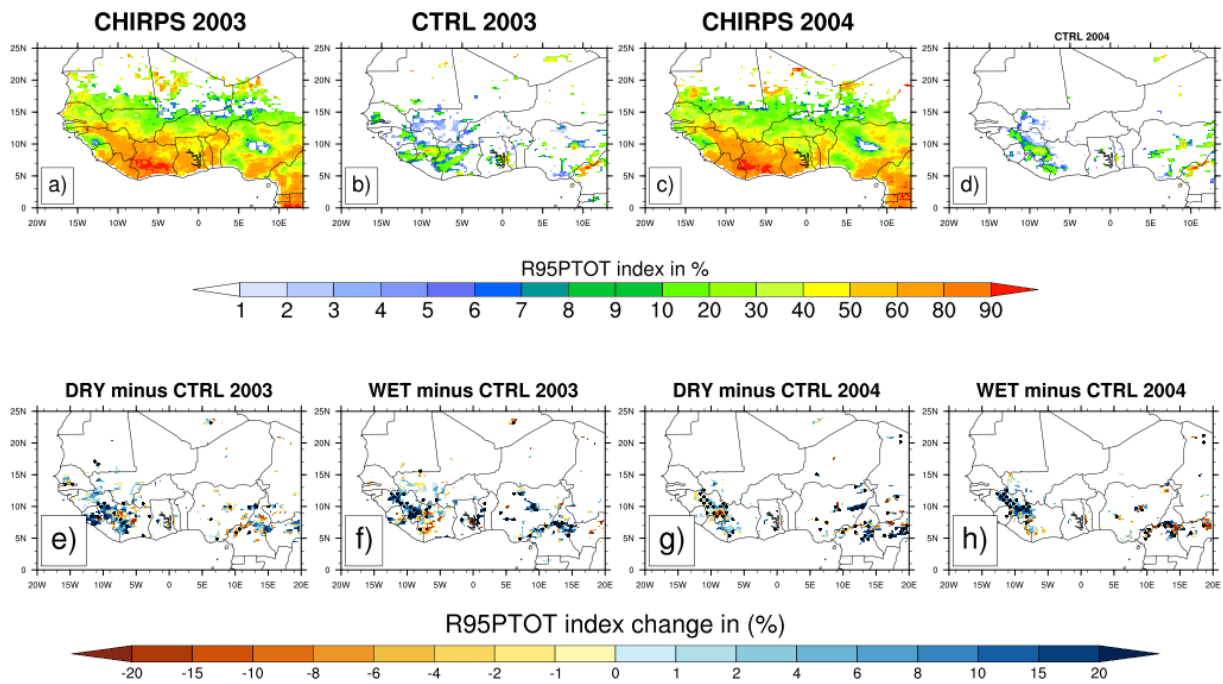
954

955



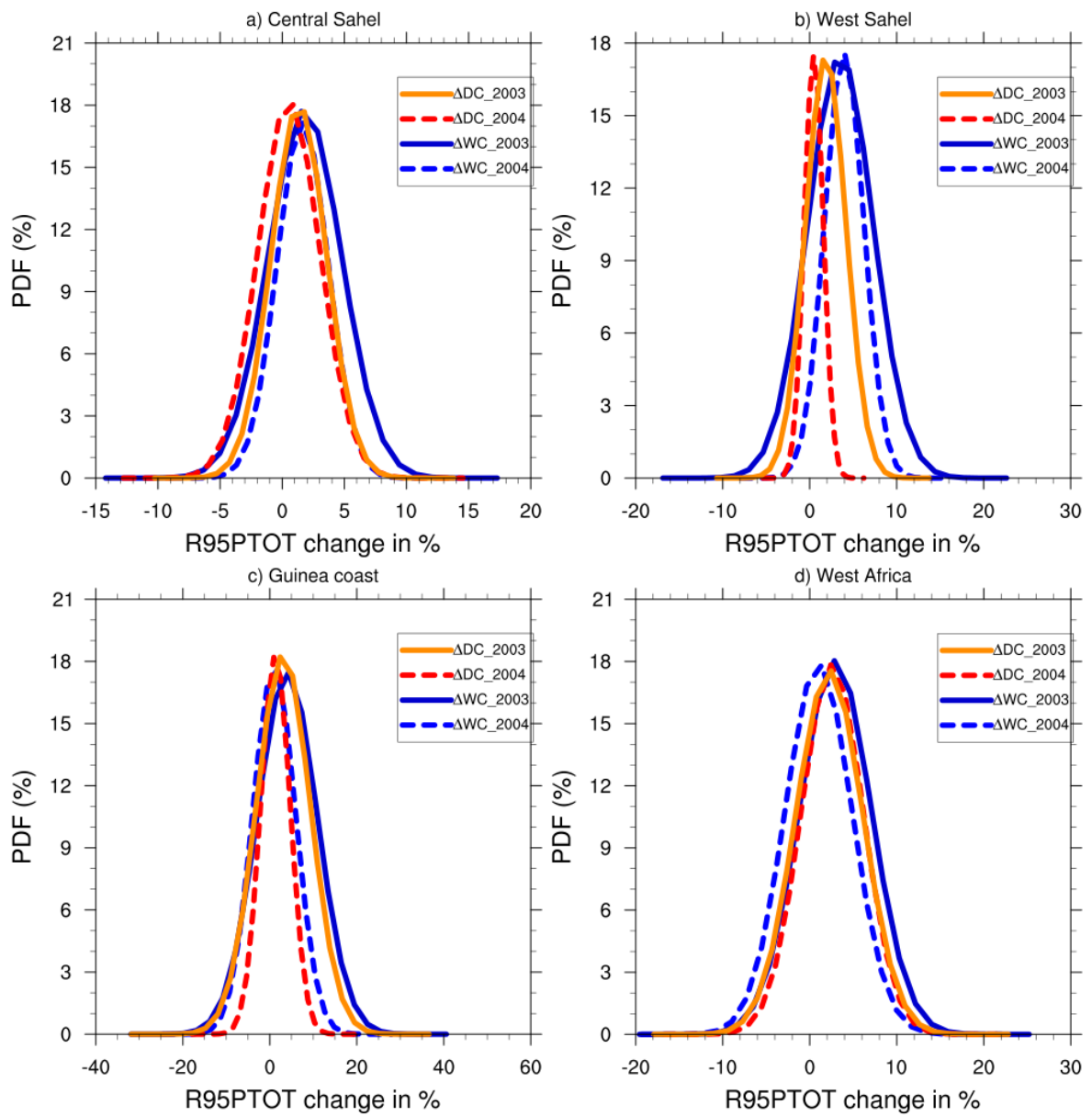
956
 957
 958
 959
 960
 961
 962
 963
 964
 965
 966
 967

Figure 11: Same as Fig. 3 but for the RX1DAY index (in mm).



968
 969
 970
 971
 972
 973
 974
 975
 976
 977
 978
 979
 980
 981
 982
 983
 984
 985
 986
 987

Figure 12: Same as Fig. 2 but for the R95pTOT index (in %).



988

989 **Figure 13:** Same as Fig. 3 but for the R95pTOT index (in %).

990

991

992

993

994

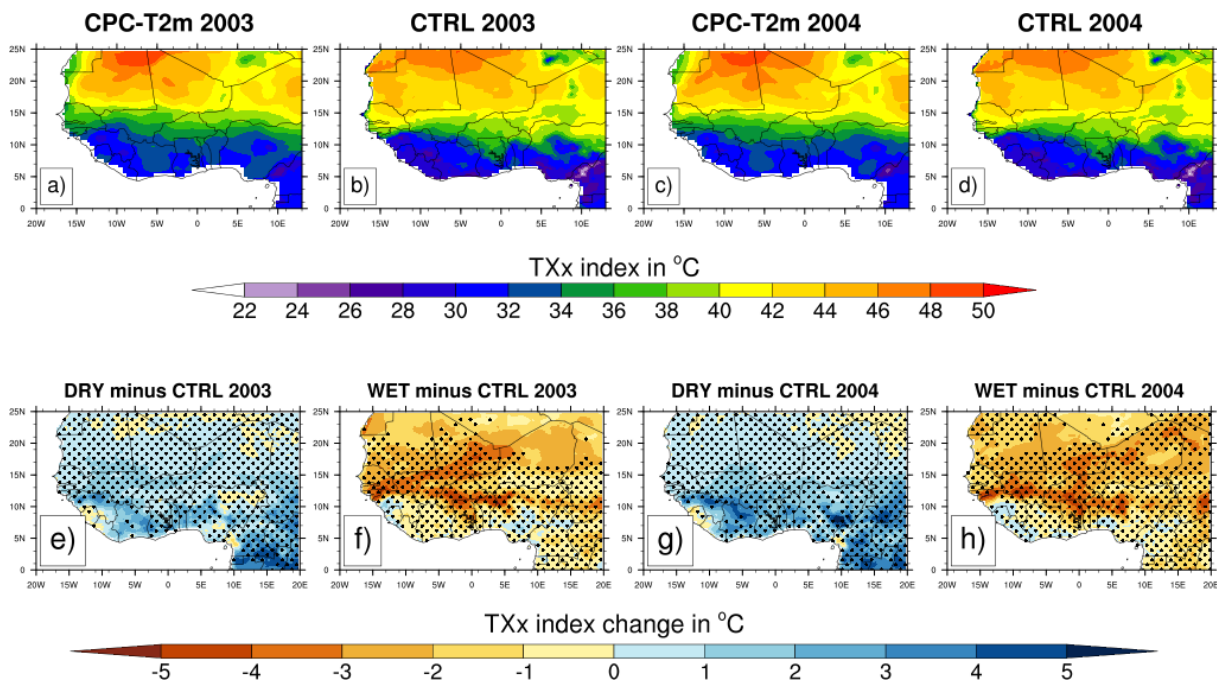
995

996

997

998

999



1000

1001

1002 **Figure 14:** The mean maximum value of daily maximum temperature (TXx index in°C) from
1003 CPC-T2m observation (a and c) for JJAS 2003 and JJAS 2004 and the simulated control
1004 (CTRL) experiments (b and d) initialized with the initial soil moisture of the ERA20C
1005 reanalysis (first panel) and changes in TXx index in°C (second panel) for JJAS 2003 and JJAS
1006 2004, from dry (e and g) and wet (f and h) experiments with respect to the control experiments.
1007 Areas with values passing the 95% significance test are dotted.

1008

1009

1010

1011

1012

1013

1014

1015

1016

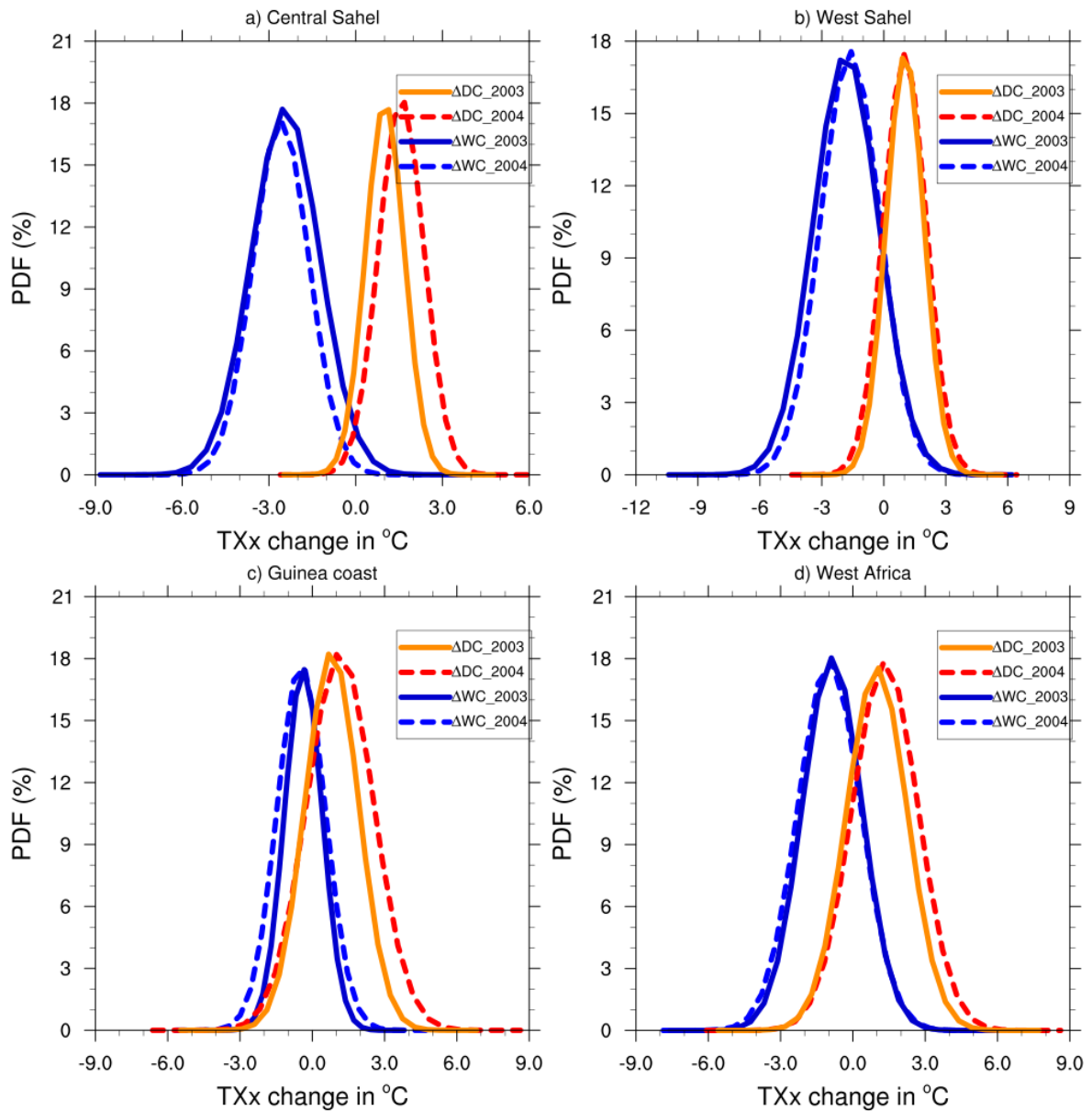
1017

1018

1019

1020

1021



1022

1023

1024 **Figure 15:** PDF distributions (%) of change in maximum value of daily maximum temperature

1025 (TXx index, in °C) for JJAS 2003 and JJAS 2004, over (a) Central Sahel, (b) West Sahel, (c)

1026 Guinea and (d) West Africa derived from dry (ΔDC) and wet (ΔWC) experiments compared to

1027 the control experiment.

1028

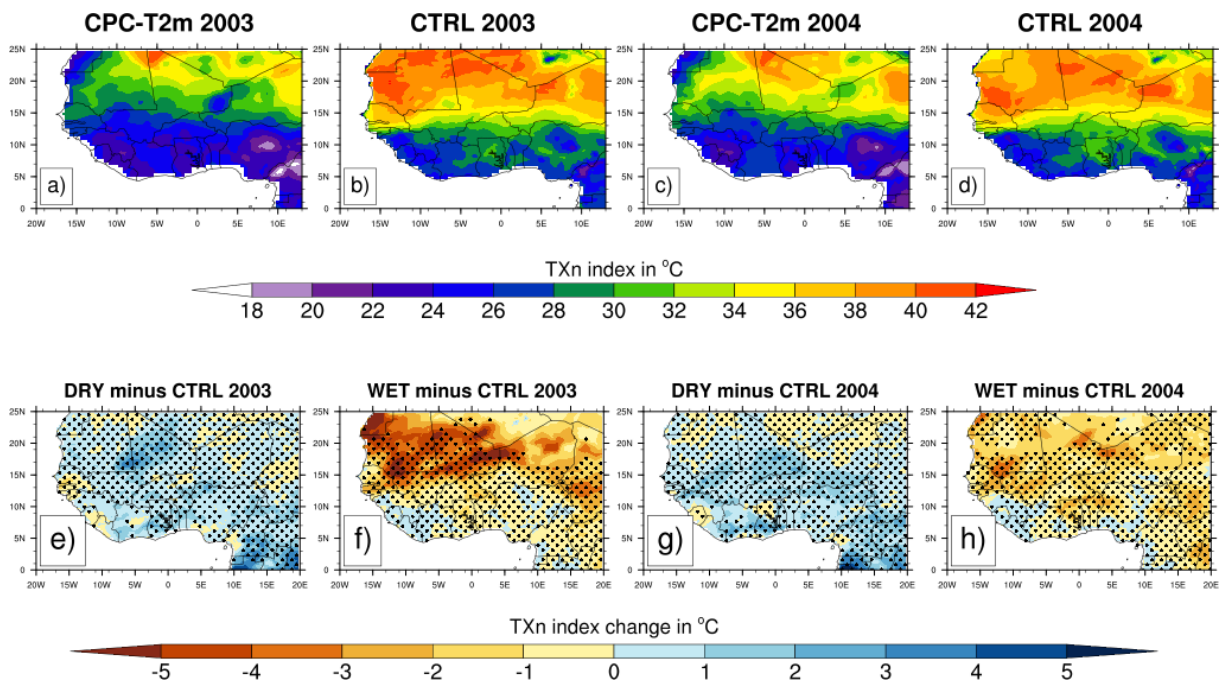
1029

1030

1031

1032

1033



1034

1035

1036

1037 **Figure 16:** Same as Fig. 14 but for the TXn index

1038

1039

1040

1041

1042

1043

1044

1045

1046

1047

1048

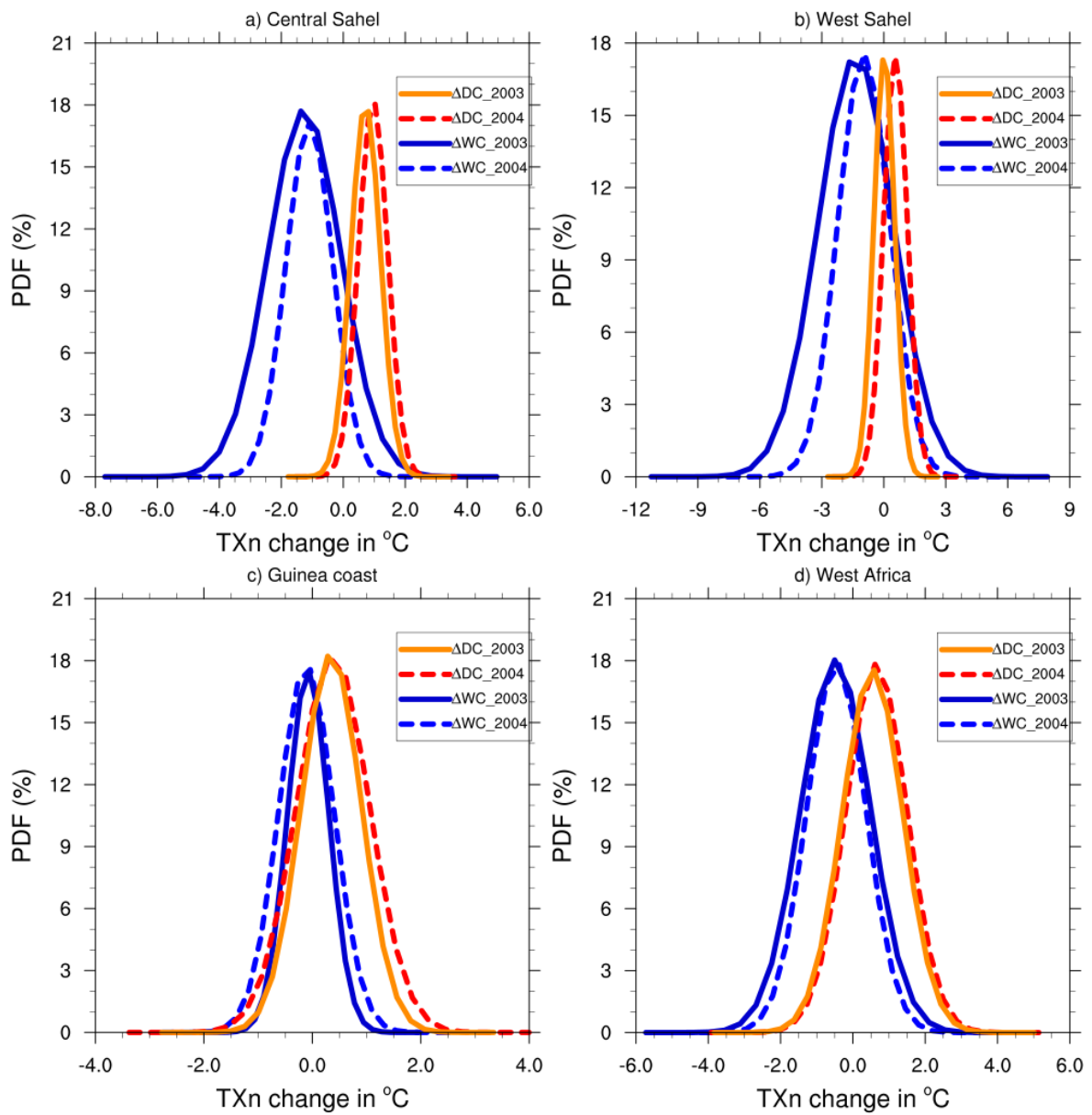
1049

1050

1051

1052

1053



1054

1055

1056

1057

1058 **Figure 17:** Same as Fig. 15 but for the TXn index.

1059

1060

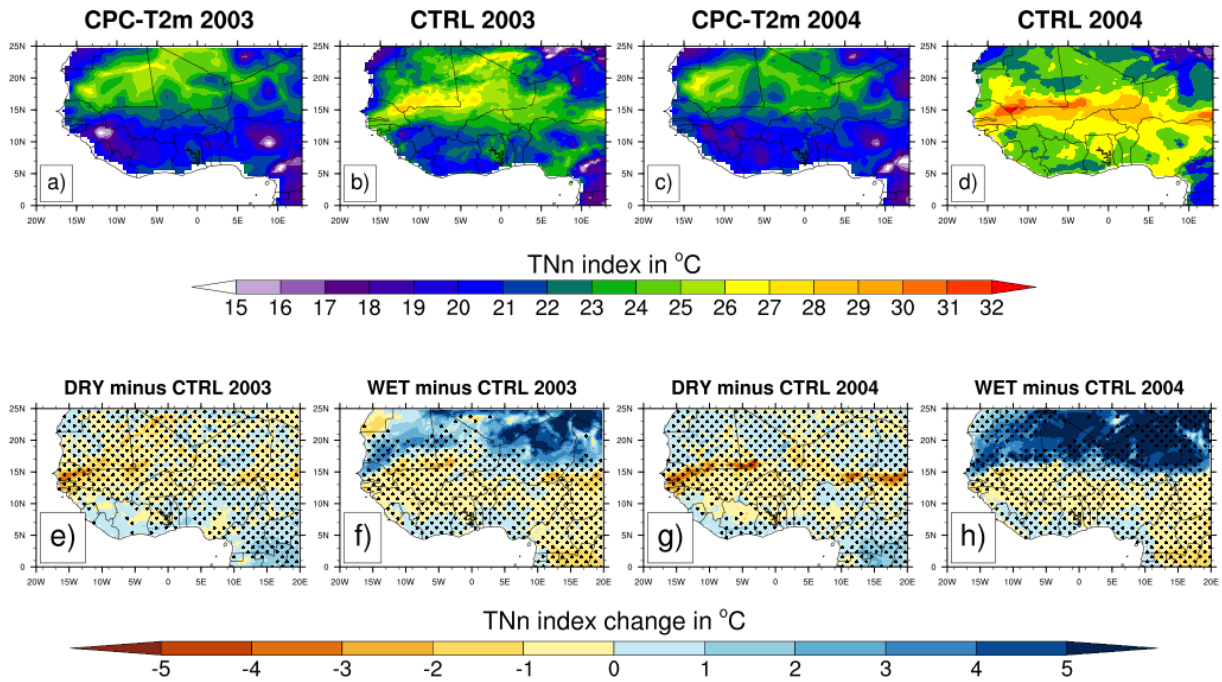
1061

1062

1063

1064

1065



1066

1067

1068

1069 **Figure 18:** Same as Fig. 14 but for the TNn index.

1070

1071

1072

1073

1074

1075

1076

1077

1078

1079

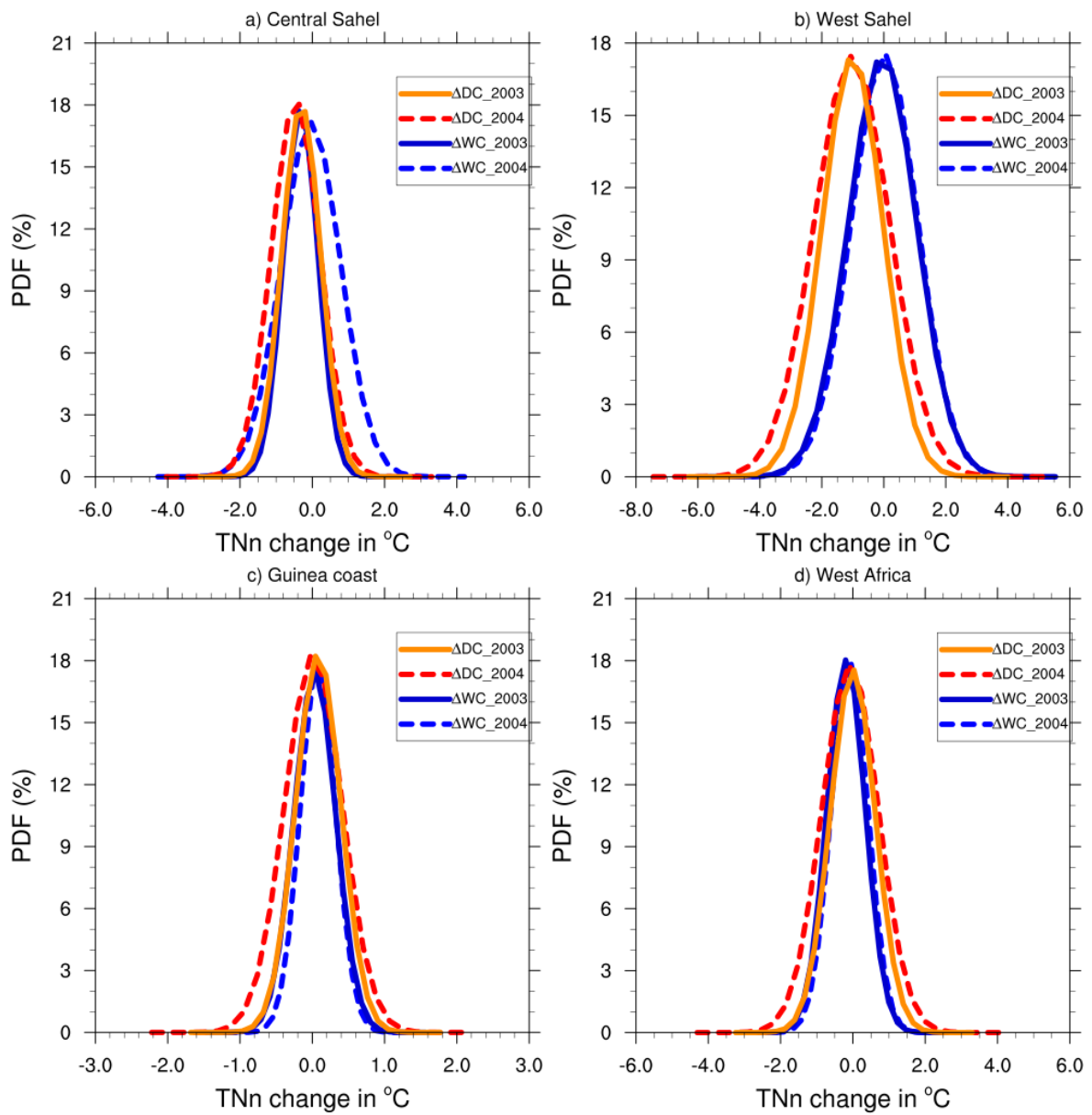
1080

1081

1082

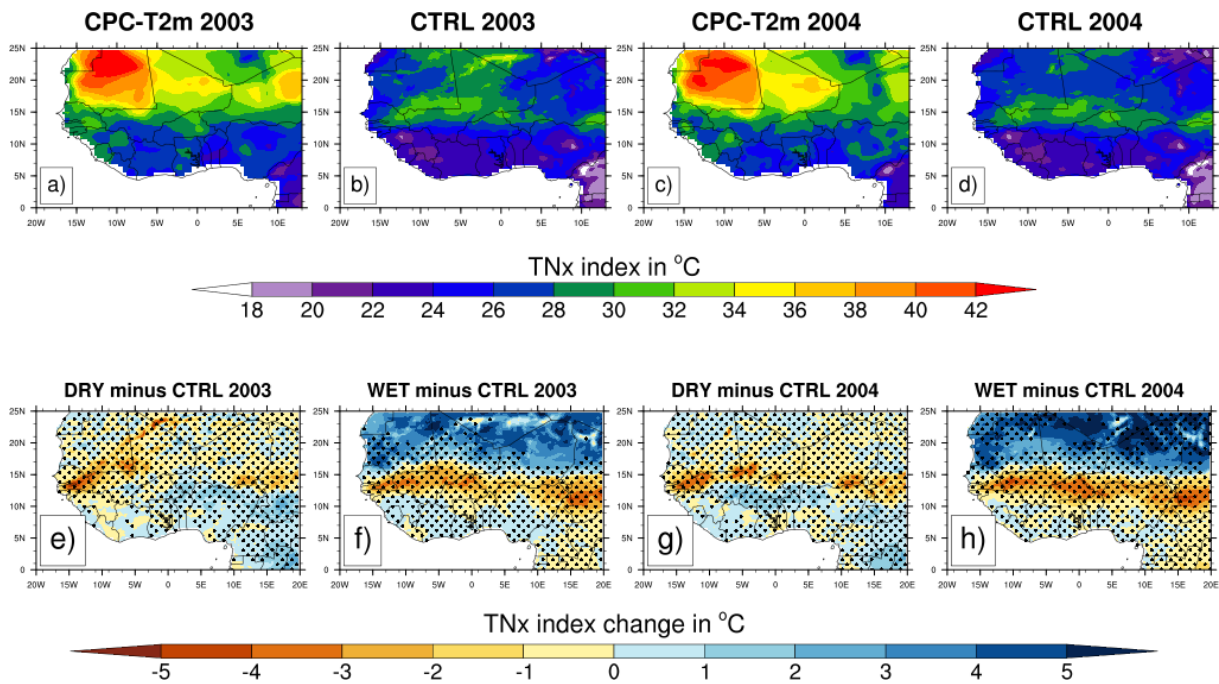
1083

1084



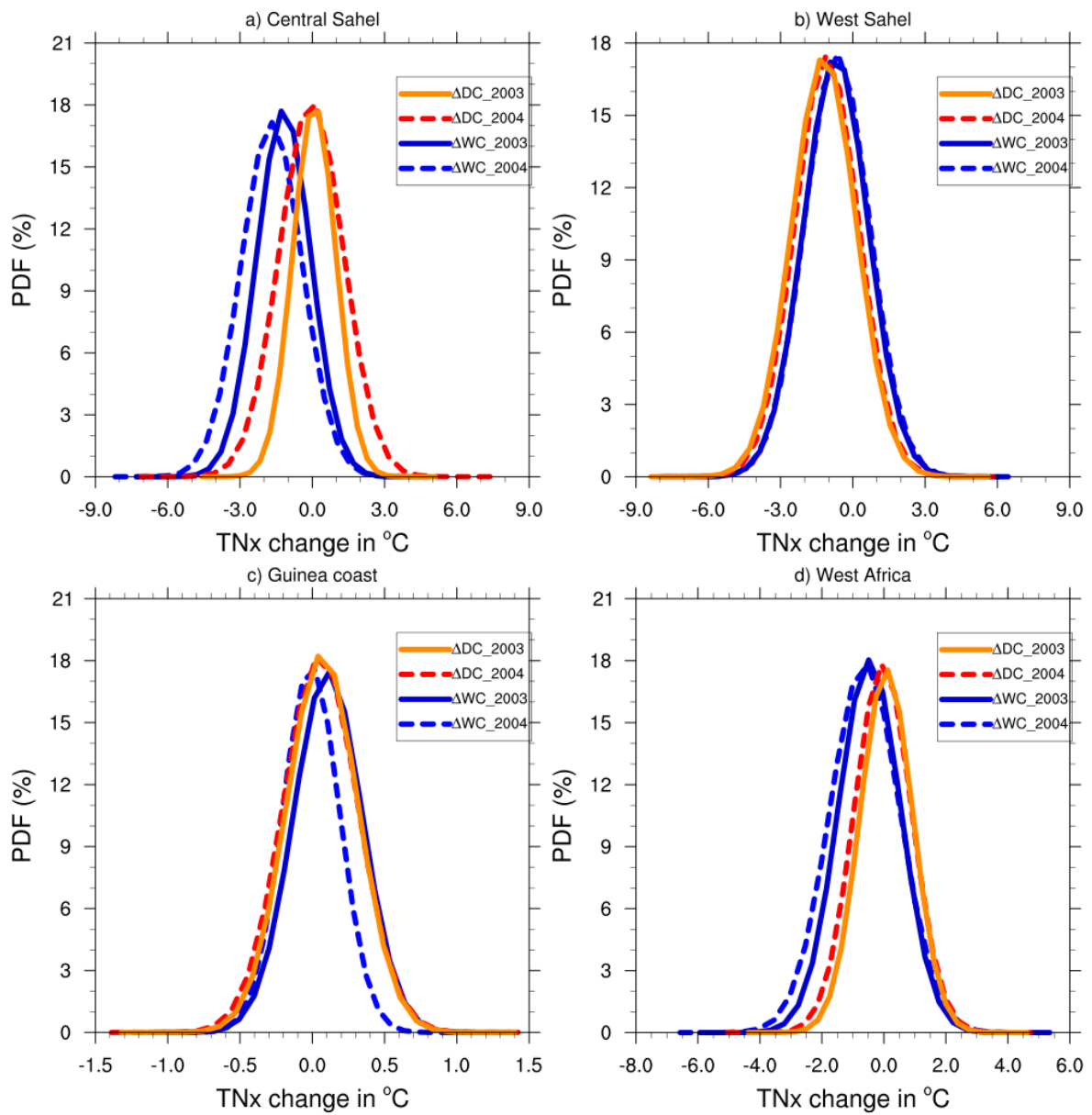
1085
 1086
 1087
 1088
 1089
 1090
 1091
 1092
 1093
 1094
 1095

Figure 19: Same as Fig. 14 but for the TNn index.



1096
 1097
 1098
 1099
 1100
 1101
 1102
 1103
 1104
 1105
 1106
 1107
 1108
 1109
 1110
 1111
 1112
 1113
 1114
 1115
 1116

Figure 20: Same as Fig. 14 but for the TNx index



1117

1118

1119 **Figure 21:** Same as Fig. 15 but for the TNx index.

1120

1121

1122